Next Materials 13 (2026) 103030

Contents lists available at ScienceDirect

Next Materials

journal homepage: www.sciencedirect.com/journal/next-materials

Research article

Thermoresponsive curcumin-loaded solid lipid nanoparticle hydrogel for periodontitis: In vitro, ex vivo, and pilot clinical evaluation

Shivam Gupta [a,1], Arashdeep Kaur [b], Joga Singh [a], Garima Sharma [a], Bakr Ahmed [a], Navjot Sharma [a,1], Pariksha Oberoi [a], Anchal Ohri [c], Aashi Bhardwaj [c], Ashish Jain [c], Praveen Rishi [b], Vishakha Grover [c], Indu Pal Kaur [a,*]

[a] University Institute of Pharmaceutical Sciences, Panjab University, Chandigarh 160014, India
[b] Department of Microbiology, Panjab University, Chandigarh 160014, India
[c] Dr. Harvansh Singh Judge Institute of Dental Sciences and Hospital, Panjab University, Chandigarh 160014, India

ARTICLE INFO

Keywords:
Antibiofilm activity
Controlled release
In-situ gelling
Rheology
Cell uptake
Cytotoxicity
Antibacterial
Solid lipid nanoparticle, Periodontitis,
Curcumin

ABSTRACT

Periodontitis (PD) is a chronic inflammatory disease caused by oral dysbiosis, aggravated by oxidative stress, leading to gum recession, periodontal pocket formation, clinical attachment loss, alveolar bone loss and eventually tooth loss. Curcumin, possesses antioxidant, antimicrobial, and anti-inflammatory properties making it suitable for periodontitis control, but its clinical efficacy is limited by poor solubility and instability. Curcumin-loaded solid lipid nanoparticles (C-SLNs), previously optimised to improve solubility, stability, and permeability, were formulated for periodontal pocket application. C-SLNs showed 62.8–83.9% in vitro biofilm inhibition against clinical sub-gingival plaque isolates, at 1500 and 2000 μg/mL, respectively. EPS matrix fragmentation, dispersion and bacterial cell lysis were observed in biofilms grown ex vivo on dentine discs treated with 1500 μg/mL of C-SLNs, indicating biofilm penetration. Confocal microscopy showed a 38-fold greater cellular uptake of fluorescein isothiocyanate loaded F-SLNs than free fluorescein isothiocyanate in human epithelial carcinoma cells. The C-SLNs dispersion was lyophilized and incorporated into a thermoresponsive Carbopol–poloxamer hydrogel to improve its structural integrity, adhesion, and retention in periodontal pockets. C-SLN hydrogel (particle size 618 nm) containing 0.6% w/v curcumin, exhibited gelation temperature of 32.7 ± 0.52 °C, acceptable syringeability and desirable consistency, > 70% cell viability and sustained release for seven days. In a randomized, parallel-arm pilot clinical trial (30 patients) C-SLN hydrogel when applied concomitantly with scaling and root planing, produced significantly greater improvements in probing pocket depth (2.7 times; $p < 0.001$) and clinical attachment level (1.5 times; $P = 0.004$) at 3 month in comparison to results at 1 month, than SRP alone treatment, supporting its potential as a non- antibiotic adjunctive strategy for periodontitis. Larger, adequately powered controlled clinical studies are however warranted.

1. Introduction

Periodontitis is a widespread chronic inflammatory disease involving the structures that support teeth such as the periodontal ligaments, alveolar bones, and gums. This condition is manifested by gum recession, formation of periodontal pockets, and bone loss, causing tooth loss [1]. It remains a significant public health concern worldwide because of the high prevalence and great contribution to oral disease burden. According to the Global Burden of Disease Study 2019, more than 1.1 billion people around the world suffer from severe periodontitis [2]. In addition, studies conducted in India have shown that about 47.2% of the population has periodontitis, with 17% presenting severe forms. A regional study carried out in the state of Tamil Nadu found that 47.7% had periodontitis [3,4].

The pathogenesis of periodontitis is initiated by a dysbiosis of oral microflora. Pathogenic microorganisms such as *Porphyromonas gingivalis, Prevotella intermedia, Tannerella forsythia, Campylobacter rectus, Aggregatibacter actinomycetemcomitans* and Treponema strains provoke an exaggerated response from the host's immune system resulting in inflammation [5,6]. Beyond this oral condition, periodontitis is

* Corresponding author.
E-mail address: indupalkaur@pu.ac.in (I.P. Kaur).
[1] Both authors contributed equally

https://doi.org/10.1016/j.nxmate.2026.103030
Received 1 June 2026; Received in revised form 31 July 2026; Accepted 31 July 2026
Available online 8 August 2026

increasingly recognized as risk factor for systemic condition, such as cardiovascular disease, diabetes mellitus, and negative pregnancy outcomes [7].

Current treatment approaches include mechanical debridement by scaling and root planing (SRP) and, in severe cases, the use of systemic/local antibiotics as adjuncts or, in refractory cases, periodontal surgery. However, some challenges associated with this approach may include poor penetration of drugs within periodontal pockets, rapid clearance of drugs, the development of resistance, low patient compliance, and no sustained therapeutic effect. These challenges show that a material-centered approach is needed in the periodontal industry to address the customer anatomical and biochemical demands.

In recent years, inorganic and polymeric nanostructures have seen great success in the fields of environmental remediation, catalysis, and biomedical therapy with exceptional results [8,9]. These innovations are however not directly implementable in the regionally adapted dental solutions. For example, materials need to be retained at the site of need, release on demand, and be biocompatible for effective periodontal treatment. The periodontal pocket is difficult for conventional nanostructured systems to perform for a number of reasons. The combination of fast flushing caused by crevicular fluid, the irregular narrow geometry, and dense biofilm of multiple species all present unique challenges. Bridging this gap requires design of advanced material platforms that are mucoadhesive, flowable enough for application but constrained in the pocket (may be thermoresponsive) and offers sustained delivery of the active to this specific anatomical site.

Among the innovative lipid-based nanostructures, solid lipid nanoparticles (SLNs) are increasingly being acknowledged for having the capability to meet these requirements. Biocompatible solid lipid matrices, provide high drug encapsulation, protect drugs against chemical degradation, and provide controlled release behavior. These properties make them suitable for drug delivery systems. To improve the SLN performance at the target site, they can be combined with thermoresponsive polymeric hydrogel matrices. Currently, Poloxamer 407 is used as the thermogelation agent with a sol-gel transition occurring near physiological temperature (~32 °C) for convenient intra-pocket administration. Carbopol 934 adds mucoadhesive strength to hold the formulation within the periodontal pocket and adds mechanical strength. This combination of a lipid-based nanocarrier within a dual-polymer hydrogel tackles the material-level constraints of earlier nanostructured systems used for confined dental therapy.

Curcumin is a polyphenolic compound found in the turmeric plant (*Curcuma longa*) [10]. Because of its anti-inflammatory, antioxidant, and antimicrobial characteristics, curcumin is a candidate for turmeric based periodontal treatments. However, its clinical use for periodontitis treatment is limited due to poor water-solubility and rapid clearance from the periodontal pocket [11]. To address such limitations, several advanced delivery strategies based on nanotechnology have been explored, including solid lipid nanoparticles (SLNs), nanostructured lipid carriers, mucoadhesive films, and thermosensitive in-situ gels. These strategies attempt to enhance curcumin solubility, offer curcumin protection from degradation, and extend its permanence in the diseased site [12]. Researchers have investigated the use of curcumin in combination with other antimicrobial or anti-inflammatory agents to boost treatment efficacy through synergistic interactions.

Many attempts have been made to improve clinical outcomes; however, outcomes are still unpredictable and do not meet in vitro expectations because of serious issues in formulation design. Nasra et al. studied a combination of Pluronic F127 and Carbopol P934 to create a system with sustained release of curcumin for up to 168 h. Unfortunately, the system shows very high viscosities (19,000 and 37,000 cP at 4°C) and gelation at between 28°C and 34°C, making this system very difficult to work with in a clinical system [13]. Guru et al. examined a 2% turmeric nanocarrier, which was found to have antimicrobial properties like chlorhexidine. However, this formulation utilized only thermoreversible polymers that are deficient in intrinsic mucoadhesion. Thus, clinicians were required to use a physical barrier (Coe-Pak periodontal dressing) over the treated site to keep the gel from washing out. Additionally, this study also neglected the disruption of biofilm and retention for the periodontal formulation [14]. In a study by Pérez-Pacheco et al., curcumin-loaded PLGA/PLA nanoparticles were examined in a single-dose clinical model. Weak mucoadhesion and short residence time were cited as limiting factors for the treatment benefit. This was noted as the primary reason for the limited treatment benefit in their study [15]. Consequently, there remains a critical need to develop a curcumin formulation with mucoadhesive strength and prolonged retention that does not rely on external periodontal dressings.

To overcome these limitations, our study reports a unique delivery system for curcumin, where solid lipid nanoparticles (C-SLNs) have been incorporated into a thermosensitive hydrogel structure. These C-SLNs increased the solubility of curcumin up to 10,000-fold, as well as providing resistance to photodegradation, thermal degradation, and pH-induced degradation. In contrast to polymeric micelles, C-SLNs remained stable even upon autoclaving [16]. In a previous study, C-SLNs demonstrated superior antioxidant activity compared to both free curcumin and ascorbic acid, with a higher second-order DPPH radical scavenging rate constant ($k_2 = 0.00392\ (mM)^{-1}\ min^{-1}$) and a progressively lower IC_{50} over time, confirming the sustained antioxidant benefit conferred by the lipid nanocarrier system [17]. Incorporating SLNs into a hydrogel matrix effectively resolves the issues of low viscosity and insufficient retention, while ensuring extended drug release and enhanced mucoadhesion in periodontal conditions [18–20]. The thermoresponsive hydrogel is composed of Carbopol 934 and Poloxamer 407, together these polymers confers mucoadhesive strength and mechanical stability. The resulting C-SLN hydrogel consists of curcumin-loaded SLNs (which have an average diameter of ~383 nm, with a zeta potential of ~−25 mV) incorporated in a Carbopol-poloxamer hydrogel with a sol-gel transition at 32°C. Further the polymeric gel system acts as a secondary vehicle that stabilizes the SLN dispersion by reducing coalescence of SLNs upon coming close to each other [21]. The stability of C-SLNs to light was excellent; curcumin was retained at concentrations of greater than 94% in the formulation at both acidic and neutral pH; the formulation was also stable to heat and was shown to withstand sterilization by autoclaving at 121°C for 15 min [17].

The current study was therefore conceived with the objective of developing, characterizing, and clinically testing the C-SLN hydrogel formulation as an adjuvant therapeutic agent in conjunction with SRP for the management of chronic periodontitis. Extensive physicochemical characterization studies included particle size determination, zeta potential measurement, DSC, FTIR analysis, rheology, electron microscopy, and gelation. In vitro evaluation included curcumin content, release kinetics, antimicrobial activity against clinical samples of oral microflora, and cytocompatibility using human epithelial carcinoma cells (KB) cells. Upon receiving clearance from the Institutional Ethics Committee of Panjab University (PUIEC210312-III−045), clinical efficacy of developed C-SLN hydrogel was evaluated in cases of moderate to severe periodontitis patients.

The current work has the advantage in strategically integrating lipid-based nanocarriers with a finely tuned thermoresponsive polymer. To the best of our knowledge, this is one of the very early studies that specifically relate the physicochemical characteristics of curcumin-SLN hydrogel with the ex vivo multispecies biofilm abolishment and the in vivo clinical efficacy.

2. Materials and methods

2.1. Materials

Extracts of curcumin (95%), a kind gift from Sunpure Extract Pvt. Ltd., India; Compritol® 888 ATO, a sample gratefully sent by Gattefossé, France; and Phospholipon 90 G (soya lecithin), a gift from Lipoid,

Germany. Carbopol 934 was obtained from LobaChemie, an Indian company specializing in laboratory reagents and chemical products. BASF provided the reagent Poloxamer 407 for free, and all reagents used in the research were of analytical quality.

2.2. Methods

2.2.1. Spectrophotometric method of analysis for curcumin

The UV spectrophotometric method previously validated in our laboratory was used to generate a standard plot of curcumin [10]. A stock solution of curcumin at a concentration of 100 μg/mL in methanol: water (1:1) was prepared (n = 6) and used to prepare serial dilutions ranging from 0.2 μg/mL to 5.0 μg/mL. The absorbance of the prepared solutions was measured spectrophotometrically at λmax = 425 nm. The measured absorbance values were plotted against the corresponding concentrations to obtain a linear relationship. E1%1 cm, i.e., the extinction coefficient of curcumin, was calculated and used for all subsequent determinations.

2.2.2. Preparation and characterization of curcumin loaded solid lipid nanoparticles (C-SLNs)

2.2.2.1. Preparation of curcumin loaded solid lipid nanoparticles (C-SLNs). A pre-optimized formula was used to prepare curcumin-loaded SLNs by a high-pressure hot homogenization technique [16,18]. Briefly, curcumin was dissolved in polyethylene glycol (PEG) 600 (8% w/w), followed by the addition of molten Compritol® 888 ATO (5% w/w). This hot lipid phase was emulsified with an aqueous surfactant phase containing (12% w/v) Tween 80 and (0.4% w/v) Phospholipon 90 G (soya lecithin) maintained at 70°C to 75°C using a high-speed stirrer (WiseTis HD 15D, Germany) at 8000 rpm for 8 min. This coarse emulsion was then subjected to high-pressure homogenization using Emulsiflex C3 Avestin (Canada) high-pressure homogenizer at 1000 bar and three cycles to obtain a hot nanodispersion. The latter was cooled to form solid lipid nanoparticles Fig. 1.

A similar procedure was used to prepare fluorescein probe labelled SLNs (F-SLNs) using 0.002 mg/mL fluorescein isothiocyanate (FITC) instead of curcumin. The prepared FI-SLNs were dialyzed against distilled water to remove unentrapped dye. However, C-SLNs were used to maintain a total curcumin content of 6 mg/mL (entrapped and unentrapped). The prepared F-SLNs were stored at 4 °C for improved stability.

Free FITC, a dilute aqueous solution of FITC (0.002% w/v), was prepared in phosphate-buffered saline (PBS, pH 7.4) under light-protected conditions. The prepared Free-FITC was stored at 4 °C for improved stability.

2.2.2.2. Characterization of C-SLNs. Curcumin assay (total drug content, TDC): A weighed amount of C-SLNs (1 mL) was dissolved in 10 mL of a chloroform: methanol mixture (1:1) and then diluted appropriately with the selected mobile phase. The solution was analyzed spectrophotometrically at λmax = 425 nm using a corresponding blank.

$$\text{Total drug content}(\%) = \frac{\textit{Observed drug content}}{\textit{Theoretical drug content}} \times 100$$

Entrapment efficiency (EE): A dialysis membrane bag that had been soaked (overnight) in distilled water. Dialysis bags were filled with 1 mL C-SLN dispersion, sealed at both ends, and dialyzed against 100 mL of methanol at room temperature for 45 min. Methanol was selected as the dialysis medium to maintain sink conditions for free curcumin, while the practical insolubility of Compritol® 888 ATO in methanol at room temperature prevented the unwanted extraction of the entrapped drug from the intact SLNs. After the necessary dilution with methanol and chloroform (1:1), the quantity of curcumin left in the dialysis bag was evaluated using the spectrophotometric technique to quantify the amount of drug entrapped inside the SLNs. To calculate EE, the following equation was used:

$$\text{Entrapment Efficiency}(\%) = \frac{\textit{Entrapped drug}}{\textit{Total drug content}} \times 100$$

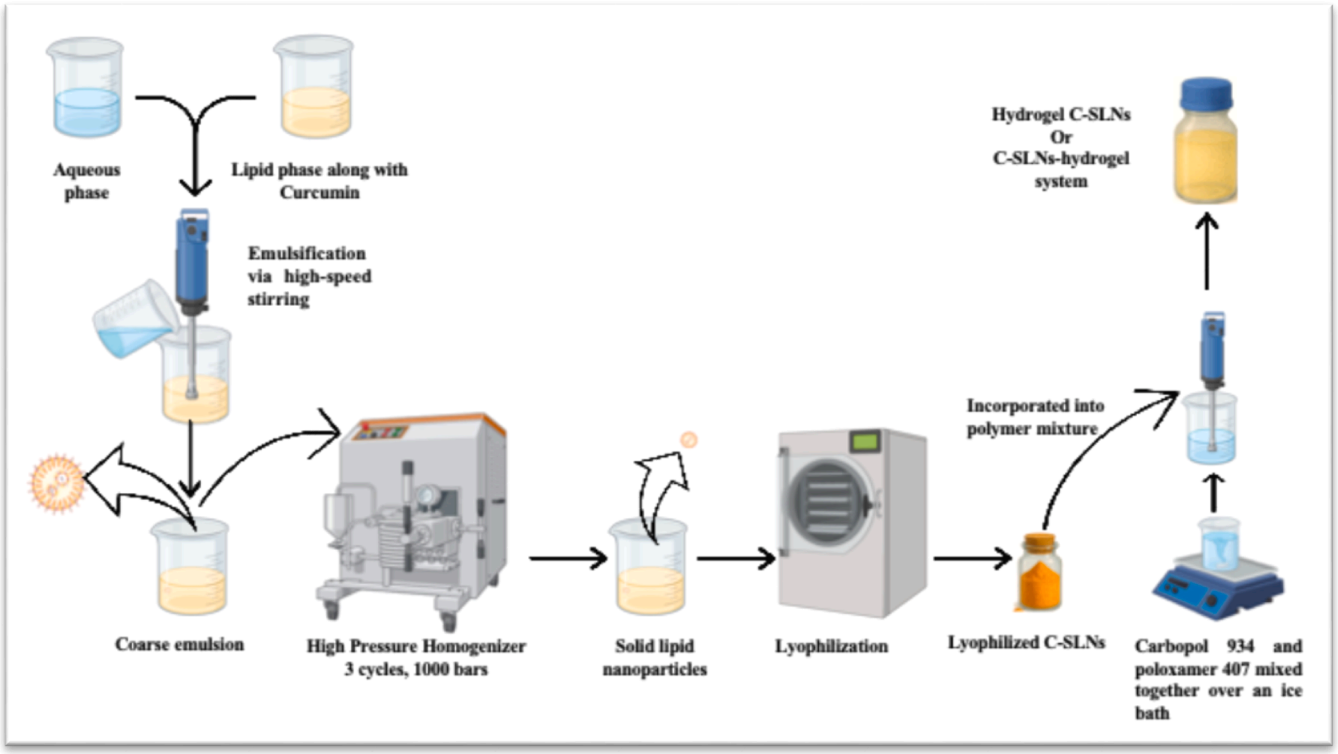

Fig. 1. Schematic diagram for preparation of curcumin-loaded solid lipid nanoparticles (C-SLN) hydrogel system.

Polydispersity index (PDI) and particle size: A Delsa TM Nano C Particle Analyzer was used to quantify the mean diameter of C-SLNs (n = 6) after the appropriate dilution (20 times) (Beckman Coulter, USA). After completion of the required dilution with double-distilled water, the particle size and PDI were determined.

2.2.2.3. Cell uptake studies. KB cells maintained in Eagle's Minimum Essential Medium (EMEM; Life Technologies) were seeded in a six-well culture plate (1×10^5 cells/well). Cells were incubated with F-SLNs or free FITC. Excess medium was washed off using phosphate buffer (pH 7.4), and the cells were then fixed with paraformaldehyde 4%. Confocal laser scanning microscopy (CLSM; Nikon Eclipse Ti2-E, Japan) was used to capture images of fluorescein isothiocyanate (FITC) and 4'-diamidino−2-phenylindole (DAPI) channels with emission maxima at 519 nm (green) and 461 nm (blue), respectively. The obtained images were processed using NIS element software [22].

2.2.2.4. Anti-biofilm activity of C-SLNs. Patient Recruitment and sample collection: Patients with periodontal disease were examined by Dr. H.S. Judge Institute of Dental Sciences and Hospital, Panjab University, Chandigarh (Institutional Ethics Committee of Panjab University (PUIEC210312-III−045), to collect tooth plaque samples. Participants were required to be above 20 years of age, have greater than 20 teeth, and have at least 8 teeth with pocket depths/attachment levels of 4 mm and above. Participants were excluded if they were pregnant or breastfeeding, underwent periodontal or antibiotic treatment in the last 3 months, had systemic conditions that may affect the periodontium (e.g. joint replacement or heart disease), had soft tissue lesions (e.g. lichen planus or leukoplakia), and if they were current smokers.

Sterile paper points were used to gather subgingival plaque samples from three patients at defined locations. For each patient, the paper points were placed in several deep gingival sulci (3–4 mm) and left undisturbed for 20 s. The plaque collected from different locations on the same patient was combined. This provided three separate patient specific samples (S1, S2, S3). These individual samples were then transported to the laboratory in buffers containing saline or reducing agents (dithiothreitol).

In vitro biofilm disruption: After culturing on various solid media, the samples were also grown on liquid culture media. Briefly, 20 μL of overnight-grown cultures was mixed with 230 μL of Tryptic Soy Broth (TSB) in the wells of a sterile polystyrene microplate. Three separate samples, labeled S1, S2, and S3, were used for growth. Broth served as the negative control. The plates were incubated at 37°C for 24 h under anaerobic conditions. Non-adherent cells were washed away with PBS (0.01 M, pH 7.0). C-SLNs were then administered to the wells at various concentrations (after washing): 1000, 1500, and 2000 μg/mL, and incubation continued at 37°C for 24 h. Untreated biofilm cells acted as controls. Samples S1, S2, and S3 were stored in wells of rows A, C, and E, respectively (see Fig. 2). Wells 1–3 in each row (A, C, and E) served as untreated controls; wells 4–6 received 1000 μg/mL of the formulation, wells 7–9 received 1500 μg/mL, and wells 10–12 received 2000 μg/mL. Fig. 2 depicts that wells 1 and 2 in Row H were designated as blanks, containing only 1% crystal violet dye. Once the treatment was completed, the contents were taken out, and the films were rinsed three times using 250 μL of phosphate-buffered saline (PBS; 0.01 M, pH 7.0). After being immersed in 250 μL of ethanol for 15 min to fix the biofilms, the microplates were subsequently drained and allowed to air-dry. After a 10-minute incubation in a 0.1% crystal violet solution (250 μL), the plates were rinsed with sterile distilled water to eliminate any excess stain and air dry again. To quantify biofilm biomass, cells that adhered to the surface bound with crystal violet and were subsequently resolubilized using 250 μL of 33% (v/v) glacial acetic acid. Independent triplicates (n = 3) were performed in all biofilm reduction experiments. A microplate reader that accurately detects high absorbances within the reader's linear dynamic range was used to measure the optical density

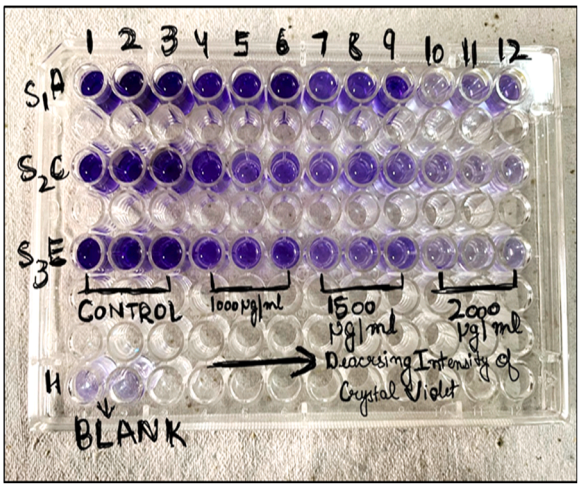

Fig. 2. 96 well plate for percent reduction in biofilm.

(OD) of the dye extracted at 595 nm. The formulation's effectiveness in removing biofilm was determined by calculating the percentage decrease in absorbance using the technique outlined by Pitts et al. [23]. The percentage reduction was calculated using the following formula:

$$\text{Percent reduction} = \{(C\text{-}B) - (T\text{-}B) - /(C\text{-}B)\} \times 100\%$$

Where B represents the average absorbance per well for the blank wells (no biofilm, no treatment), C represents the average absorbance per well of the control wells (biofilms, no treatment). T represents the average absorbance per well of the treated wells (biofilm and treatment).

Ex vivo Biofilm Disruption: An isomet low-speed saw was used to section three 2 mm-thick dentin discs from extracted human teeth obtained from patients at Dr. Harvansh Singh Judge Institute of Dental Sciences and Hospital, Panjab University, Chandigarh, India. Dentin discs were treated with 1% sodium hypochlorite (NaOCl) solution, to achieve complete sterility, for 15 min, then rinsed in sterile distilled water, and autoclaved. The specimens were placed in separate wells of six-well culture plates. To simulate a natural setting for biofilm development, 2 mL of Tryptic Soy Broth (TSB) fortified with 1% (w/v) glucose, was added to each well of the culture plates. The fortified broth aided in both the adhesion of the bacteria to the surface and the production of the bacterial extracellular polymeric matrix (EPM). Clinical plaque isolates were added to each well at the same concentration. Plates were incubated at 37°C for 24 h under anaerobic conditions. This incubation provided the conditions for the natural oral microflora to adhere to and colonize the surface of the dentin, and to complete the process of biofilm development, which included the maturation and development of a multi-species biofilm. Dentin disc was gently washed with PBS. One of the dentin discs was left untreated (control), and the remaining two were treated for 24 h with 1000 and 1500 μg of C-SLNs. Following the treatment, the test and control discs were fixed for 2 h in 2.5% glutaraldehyde. The glutaraldehyde was then washed three times with 0.1 M PBS, pH 7.2. After fixation, each gradient was gradually dehydrated for approximately 15 min with incremental concentrations of ethanol (30–90%). At room temperature, 100% ethanol was used for the final dehydration. The dehydrated samples were dried and examined by FE-SEM.

2.2.3. Preparation of C-SLNs loaded into Hydrogel system

2.2.3.1. Lyophilization of C-SLNs. The C-SLNs were autoclaved at 121 °C for 15 min to obtain a sterile dispersion. After removal from the autoclave, the dispersion was shaken gently to redisperse uniformly and then cooled to room temperature for the reformation of SLNs. Sterile C-

SLNs were weighed and frozen overnight, after which they were lyophilized for two cycles in a lyophilizer (alpha 2–4 LDplus) [17]. Lyophilization served to remove excess water and concentrate the C-SLNs for subsequent incorporation into the hydrogel.

2.2.3.2. Hydrogel Preparation. The cold method was used to prepare Carbopol-poloxamer gel [24]. First, a magnetic stirrer was used to dissolve Carbopol 934 in deionized water at room temperature. After complete dissolution, the solution was chilled in an ice bath and then Poloxamer 407 was added slowly with constant stirring. The mixture was cooled at 4 °C for 24 h to achieve full wetting/solution and release of trapped air bubbles. The polymer solution was autoclaved and refrigerated until use.

2.2.3.3. Incorporation of lyophilized C-SLNs. The lyophilized C-SLNs (amounts corresponding to 0.6 mg curcumin/mL for Formulation A and 1 mg curcumin/mL for Formulation B) were gradually added to the prepared polymeric solution (Carbopol 934 and Poloxamer 407) and mixed at 5000 rpm for 10 min using high-speed stirring (WiseTis HD 15D, Germany). The resulting C-SLN-hydrogel (A and B) was stored in amber bottles at 4°C Fig. 1.

2.2.4. Hydrogel characterization

Total drug content [TDC]: The gel was dissolved in 10 mL of methanol. Spectrophotometric analysis of the produced solution was performed at λmax = 425 nm, with methanol as a blank. TDC was determined using the previously mentioned equation.

Polydispersity index (PDI) and particle size: Using a DelsaTM Nano C Particle Analyzer, the PDI and mean particle size of formulations A and B (six samples each) were calculated after the formulations were appropriately diluted (100 times) with double-distilled water (Beckman Coulter, USA).

pH: The pH of each formulation was measured in triplicate at 4 °C (mimicking controlled storage conditions) using a calibrated pH meter, and results are reported as mean ± SD.

Autoclavability: Autoclavability of the curcumin-loaded solid lipid nanoparticle (C-SLN) hydrogel was evaluated by subjecting aliquots (n = 3) to a saturated-steam sterilization cycle at 121 °C for 15 min (≈15 psi), followed by controlled depressurization and cooling to ambient temperature; matched, non-autoclaved samples stored at room temperature served as process controls.

Syringeability: A 21-gauge needle syringe was filled with one mL of the cold gel, and its flow characteristics were assessed under normal handling pressure [25]. The test was performed for plain hydrogel in addition to formulations A and B.

Gelation temperature: A 10 mL sample of Formulation A was delivered to a 20 mL beaker under magnetic stirring to measure the gelation temperature. By gradually increasing the temperature of the sample by 1 °C/min, the gelation temperature was determined as the point at which the magnetic bar met the motion resistance. The temperature at which the gel formed was verified by inverting the container.

Texture profile analysis: To determine the mechanical properties of the formulations system, a software-controlled penetrometer and texture analyzer (Stable Micro Systems, Surrey, UK) were used. The formulation was delivered to a bottle, subjected to a 20-minute ultrasonic water bath to remove air bubbles, and then the temperature was maintained at 37 °C. The probe was compressed at a preset rate of 2 mm s^{-1} into the CSLN *in situ* gel. Estimated various mechanical parameters of the gel formulation, viz., compressibility, adhesiveness, cohesiveness, and hardness. The test was performed for C-SLNs, plain hydrogel, and formulations A and B.

FE-SEM: Field emission scanning electron microscopy (FESEM) was performed using a Hitachi H100 system. Samples were sputter-coated with a 5 nm platinum layer and placed on carbon-coated copper grids. Images were captured at magnifications of 10.0Kv to visualize fine morphological features.

In vitro drug release: The in vitro release behaviour of curcumin from Formulations A and B was evaluated using a dialysis-bag method under sink-maintaining, hydro-organic conditions. Briefly, pretreated dialysis tubing (12–14 kDa MWCO) was cut into 10 cm lengths, soaked in distilled water for 30 min, rinsed with methanol: water (1:1, v/v) release medium, and equilibrated for 15 min. Each sample, exactly 1 mL, was introduced separately into dialysis bags that were sealed at both ends to avoid air bubble formation. Each bag was put in a 50 mL release medium containing methanol and water in equal proportions. The medium was kept at 37.0 ± 0.5 °C and stirred at 80 rpm. The choice of a 50% methanol concentration was driven by several considerations, namely, to provide sink conditions for poorly soluble curcumin, prevent curcumin from aggregation and precipitation, minimize the effect of hydrolysis on curcumin, and provide accurate quantification by absorption at 425 nm [16,17]. Samples (2 mL) were withdrawn from each solution at specified intervals (0.5, 1, 2, 4, 6, 8, 12, 24, 36, 48, 60, 72, 96, 120, 144 and 168 h) and replaced with a freshly pre-warmed medium. All samples were kept in the dark in amber bottles at 4 °C and analyzed within 24 h. The concentration of curcumin was determined by using a spectrophotometer with the use of a validated calibration curve ($r^2 \geq 0.999$) established in a mixture of methanol: water (1:1). The cumulative release was calculated by considering the volumes of samples withdrawn and replaced and was expressed as percentage of the initial curcumin amount. Each formulation was tested in six replicates, with the outcomes expressed as mean ± SD. These results were analysed using zero-order, first-order, Higuchi, Korsmeyer-Peppas, and subsequently the Weibull model to elucidate the release mechanism. Statistical comparisons were made using f1/f2 factors and ANOVA ($p < 0.05$) to evaluate differences between formulations.

In vitro cytotoxicity: Formulation A was assessed for its cytotoxic potential using the KB cell line (human epithelial carcinoma cells). The KB cell line, derived from the oral cavity, was selected as an in vitro model owing to its relevance to the oral epithelial tissues encountered in periodontal pockets. This model is widely used for evaluating the mucosal safety of local drug delivery systems and provides a predictive assessment of potential cytotoxic effects before in vivo studies. KB cell viability was investigated after exposure to free curcumin, C-SLNs, and Formulation A for 24 h. The selected concentrations of curcumin were 20 and 40 μg/mL. MTT (3-(4,5-dimethyl−2-thiazolyl)−2,5-diphenyl-2H-tetrazolium bromide) at 2.5 mg/mL per well was used to assess cytotoxicity. Cells (1×10^5) were grown in EMEM supplemented with 10% fetal bovine serum (FBS; Life Technologies) and 1% v/v penicillin-streptomycin (P/S; Sigma Aldrich) in a 96-well assay plate. Absorbance was measured at 570 nm using a Gen 5 plate reader (BioTek, Winooski, VT, USA), with background correction performed by subtracting the absorbance at 690 nm from that at 570 nm [22].

2.3. Clinical study design

A prospective, randomized, open – label, parallel-arm pilot clinical trial was conducted to evaluate the preliminary clinical efficacy, safety, and feasibility of a curcumin-loaded solid lipid nanoparticle (C-SLN) hydrogel as an adjunct to SRP in patients with moderate-to-severe generalized chronic periodontitis. The study was not designed or powered to establish definitive treatment superiority but rather to generate initial estimates of treatment effect, variability, participant recruitment and retention, and intervention feasibility to inform the design and sample size calculation of future adequately powered randomized controlled trials. This approach is consistent with the recommendations of the CONSORT 2010 Extension for Randomized Pilot and Feasibility Trials, which recognizes pilot studies as an essential step in evaluating the practicality and methodological robustness of novel therapeutic interventions before undertaking confirmatory clinical trials.

The study protocol was reviewed and approved by the Institutional Human Ethics Committee, Panjab University (Approval No.

PUIEC210312-III−045) and was conducted in accordance with the ethical principles of the Declaration of Helsinki. Written informed consent was obtained from all participants prior to enrolment after explaining the study objectives, procedures, potential benefits, and possible risks.

Thirty patients diagnosed with moderate-to-severe generalized chronic periodontitis were screened for eligibility according to the predefined inclusion and exclusion criteria. Eligible participants underwent comprehensive periodontal examination, and detailed medical and dental histories were recorded before enrolment.

Following baseline examination, participants were randomly allocated in a 1:1 ratio to either the experimental or control group using computer-generated random sequence. Due to the open-label design of the study, formal allocation concealment was not employed. However, all clinical outcome measurements were assessed by an independent, blinded, and calibrated assessor to mitigate assessment bias.

Fifteen participants were allocated to each treatment group: control group (n = 15): SRP alone and experimental group (n = 15): SRP followed by subgingival application of the optimized C-SLN hydrogel (equivalent to 0.6% w/v curcumin). No participants crossed over between treatment groups.

Due to the nature of the intervention, operator blinding during treatment administration was not feasible. All clinical measurements were, however, recorded by a second assessor who was blinded to treatment group allocation and had no role in participant recruitment, randomization, or intervention delivery. Prior to study initiation, examiner calibration was conducted on patients not enrolled in the study using standardized periodontal probing techniques, with repeated measurements obtained to confirm consistency in probing depth (PD) and clinical attachment level (CAL) recordings. This separation of role was implemented to minimize measurement bias and improve the reliability and objectivity of the clinical findings.

All participants received full-mouth SRP using standard periodontal instrumentation. In the experimental group, the C-SLN hydrogel was administered immediately following completion of SRP at the baseline visit.

The C-SLN hydrogel was delivered into the periodontal pocket using a blunt-tipped cannula inserted to the base of the periodontal pocket and withdrawn gradually while dispensing the formulation until the material reached the gingival margin, ensuring complete filling of the periodontal pocket. No additional applications of the hydrogel were performed during the three-month follow-up period. The primary clinical outcome measures were Probing Pocket Depth (PD) and Clinical Attachment Level (CAL), recorded at Baseline, one month, and three months using a standardized UNC−15 periodontal probe at six sites per tooth by a calibrated examiner.

Participants were evaluated at each follow-up visit for treatment-related adverse events, including pain, swelling, allergic reactions, local irritation, delayed wound healing, infection, abscess formation, or any other unexpected complications. No serious adverse events attributable to the investigational hydrogel were observed during the study period.

Data were analyzed using SPSS version 20 (IBM Corp., Armonk, NY, USA). Continuous variables are expressed as mean ± standard deviation. The normality of data distribution was assessed using the Shipro-Wilk test. As the data were not normally distributed, intragroup comparisons across time points were performed using the Wilcoxon signed-rank test, and intergroup comparisons at each time point were performed using the Mann–Whitney *U* test. Statistical significance was established at $p < 0.05$.

3. Results and discussion

3.1. Spectrophotometric method for curcumin analysis

A standard curve of curcumin was constructed in the range of 0.2–5 μg/mL in methanol: water (1:1), with an $E^{1\%}1$ cm value of 1357. Curcumin was analyzed spectrophotometrically at a λmax of 425 nm.

3.2. Characterization of C-SLN

C-SLNs showed a high assay of 98 ± 2.56% / (5.88 ± 0.05 mg/mL; n = 6) and a significant entrapment efficiency of 74.67 ± 2.38% (n = 6). The average size of the C-SLN particles was 383 ± 34 nm (n = 6) with a low PDI of 0.167 ± 0.052, indicating good monodispersity of the samples. The high entrapment efficiency reflects effective encapsulation of the hydrophobic curcumin within the solid lipid core, while the nanoscale dimensions and low PDI are consistent with a well-controlled preparation process and are well within the range considered optimal for periodontal pocket penetration.

3.3. Cell uptake studies

F-SLNs and C-SLNs, with payload of fluorescein and curcumin respectively, have same lipid matrix, similar size (361 ± 31.7 nm, PDI 0.214 ± 0.25), surface chemistry and preparation methods. As FITC is lipophilic like curcumin, it will also be incorporated in the lipid core, internalized into cells by the same pathways and also follow similar intracellular trafficking. These observations make F-SLNs a good surrogate marker for C-SLNs. Presently a semi-quantitative image analysis of a set of representative confocal fields, using ImageJ (Fig. 3), provided an estimated fluorescence of ~0.91 AU for F-SLN treated cells and ~0.024 AU, correspondingly for cells treated with free FITC. Whereas the specific image analysis (as a representative observation) was not aimed to provide a statistical p-value, the data indicates that cellular internalization of F-SLNs was approximately 38 times greater than that of free FITC. This large relative difference (both visually and in a quantitative sense) reflects that SLNs mediate high endocytic uptake of their cargo. This 38-fold enhanced cellular uptake represents a critical biopharmaceutical advantage over conventional free-curcumin systems, which rely on passive diffusion and exhibit limited intracellular accumulation; a recognized limitation of previously described thermoresponsive curcumin formulations [13].

3.4. Anti-biofilm activity of C-SLNs

Prior to calculating the percentage reduction, the absolute optical density (OD) for the untreated control biofilms was recorded. The control samples showed a significant amount of biofilm, with absolute OD values of 2.78–3.50. This provided a strong baseline biofilm, which the treatments were able to eliminate in a dose-dependent manner.

Consistent with a dose-response, all three patient samples (S1-S3) showed an inhibitory response to the treatments. A maximum treatment concentration of 2000 μg/mL reached a mean percent reduction of 92.2% (S1), 83.1% (S2), and 76.4% (S3). These results indicate near-complete inhibition of S1 with a strong inhibitory response for S2 and S3. When the treatment concentration was decreased to 1500 μg/mL, the observed reductions were 69.1% (S1), 71.2% (S2), and 48.0% (S3). The lowest treatment concentration of 1000 μg/mL exhibited mean percent reductions of 34.9% (S1), 26.8% (S2), and 34.0% (S3), respectively which though modest are still significant (Fig. 4). The error bars indicate the acceptable variability and confirm that higher concentrations consistently decreased the bacterial count.

The varying levels of biofilm reduction among the three clinical samples demonstrate the variation often observed in periodontal disease. The subgingival microbial community is polymicrobial and encased in a protective EPS matrix that varies in composition among individuals and may be quite thick. For example, S3, which had a 2000 μg/mL treatment reduction of 76.4%, likely has a more protective or dense EPS matrix than S1, which showed a reduction of 92.2%. The results demonstrate the translational significance of C-SLNs, as a novel yet effective option withstanding inter-patient microbial variability.

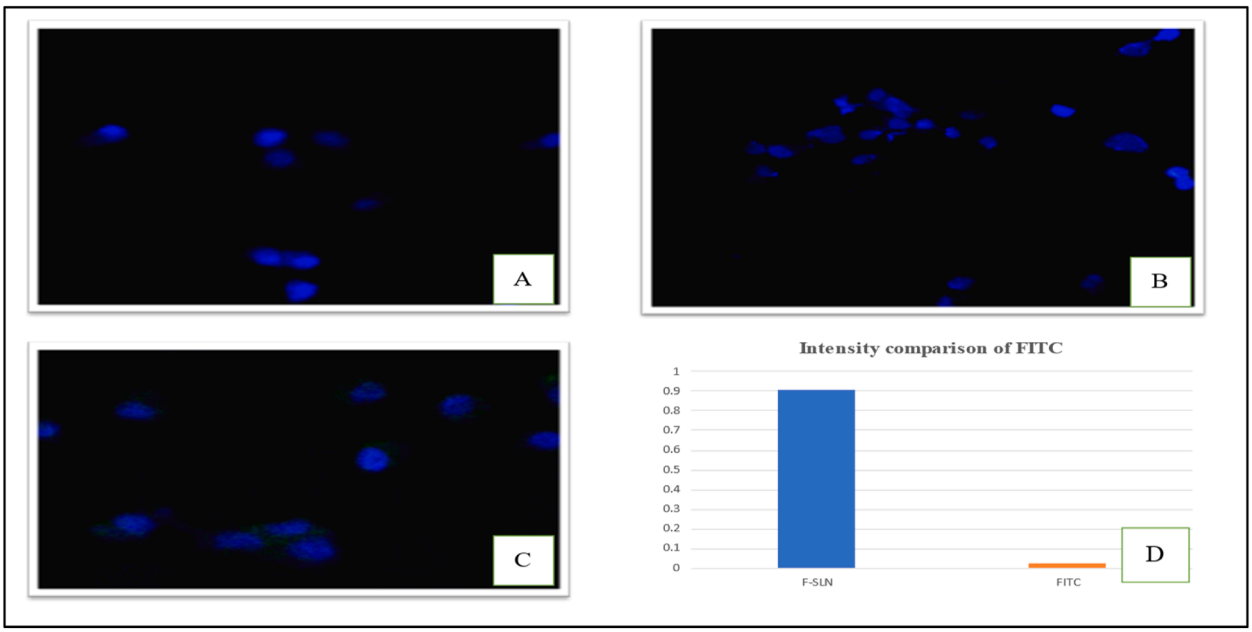

Fig. 3. Cell uptake experiments. A: control cell nuclei stained with DAPI; B: cells labeled with free FITC where no green fluorescence was observed; C: cells labeled with F-SLNs where green fluorescence was present; D: comparison of fluorescence intensity after 24 h in cases B and C using ImageJ software. The blue color of DAPI was incorporated into the nucleus of the cell; FITC is indicated as green fluorescence.

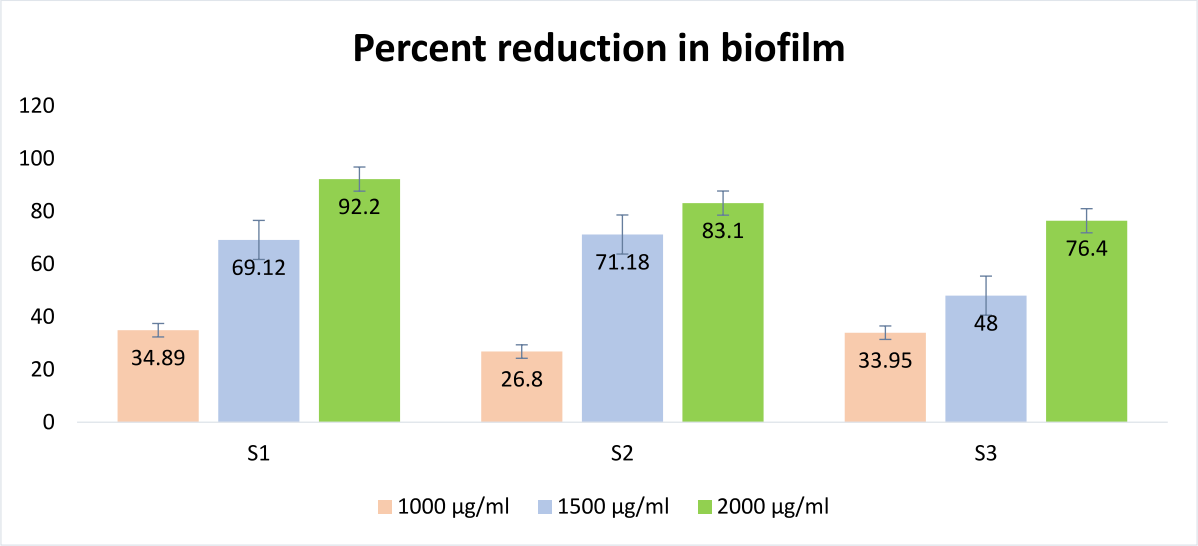

Fig. 4. Percent reduction in biofilm at 1000, 1500, and 2000 µg/mL across S1-S3 (mean±SD, n=3; independent replicates). From the one-way ANOVA, there were significant differences among the groups, $F(8,45) = 206.09$, $p < 0.0001$. From Tukey's HSD test at each station, all pairwise comparisons showed statistical significance ($p < 0.0001$) with larger concentrations having a greater effect on the reduction in biofilm.

3.4.1. Biofilms on the tooth surface

Fig. 5 represents the macroscopic appearance of the human teeth samples after two days of biofilm formation followed by the treatment. In the case of the "Control" well (right upper corner), there is the formation of dense and opaque biofilm on the enamel surface. The "Contaminated" tooth (middle part) shows prominent biofilm growth without any treatment. Treatment with C-SLNs at a concentration of 1000 µg/mL results in significant clearing of the medium, which consequently leads to the tooth returning to its original appearance and suggests a substantial reduction in the amount of biofilm. A dose of 1500 µg/mL (lower right corner) leaves the surface nearly intact.

Fig. 6 shows high-resolution FESEM pictures of these samples. In A-C panels (controls), a continuous, multilayered biofilm composed of closely packed cocci and rods of bacteria surrounded by a dense EPS network is observed. Bacterial cells have a consistent size of 0.5–1 µm, look swollen and interconnected with filamentous structures made up of EPS. On the other hand, D-E panels (1000 µg/mL treatment) show damage in terms of fragmentation of the EPS network, separation of the clusters by empty spaces, membrane blebbing and partial cell collapse. F-G panels (1500 µg/mL) depict evident morphological destruction of the cells in terms of wall rupture, cytoplasm leakage and deflation, resulting in fewer intact cells. Panel H shows (uncoated tooth surface after harvesting) that the biofilm structures shown in A-C panels cannot be produced via any artifacts associated with sample preparation. Thus dose-dependently, C-SLNs show fragmentation and dispersion of the EPS matrix at 1000 µg/mL, whereas at 1500 µg/mL, bacteriolysis is evident.

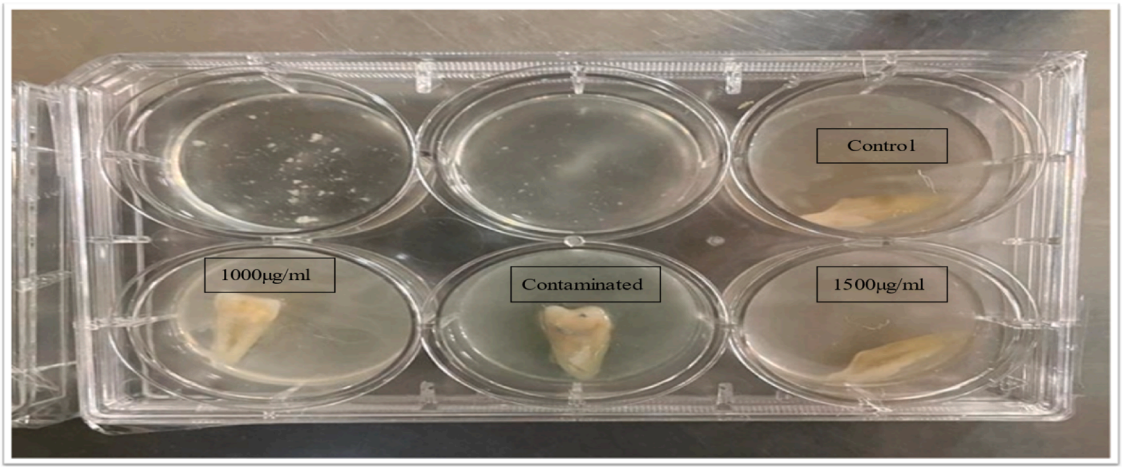

Fig. 5. Macroscopic view of tooth specimens following 48 h biofilm formation and C-SLN treatment. Upper row: Control (no treatment) and contaminated specimens display dense, opaque biofilm coatings. Lower row: Treatment with 1000 µg/mL C-SLNs markedly clears the biofilm, while 1 500 µg/mL C-SLNs restores near-pristine enamel appearance.

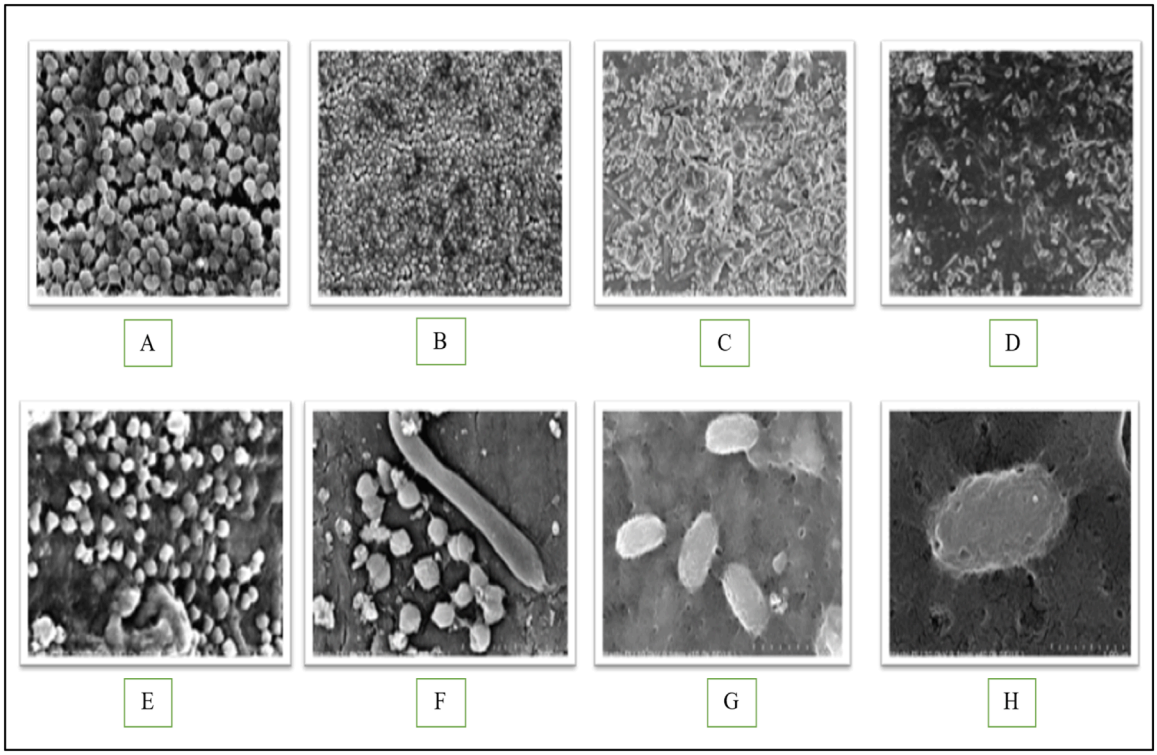

Fig. 6. FESEM micrographs of biofilm architecture and C-SLN-induced disruption. A-C: Untreated control biofilm shows multilayered cocci and rods enmeshed in thick EPS. D-E: 1000 µg/mL C-SLNs fragment the EPS matrix, disperse microcolonies, and induce membrane blebbing. F-G: 1500 µg/mL C-SLNs produce extensive cell-wall rupture, cytoplasmic leakage, and deflated bacterial cells. H: Cleaned tooth surface control confirming absence of preparation artifacts.

This combination of matrix disorganization and cellular damage indicates that C-SLNs penetrate the biofilm successfully offering an antimicrobial defence barrier.

Recent multidisciplinary literature suggests that advanced functional materials coupling their properties with application performance have a great biomedical potential. The present research thus exemplifies that structural traits of successfully designed C-SLN hydrogel fulfills the expectations of an advanced functional nanomaterial as dictated by its performance in periodontal applications [26,27]. The nanoscale dimensions of C-SLNs allow it to penetrate the EPS matrix of biofilms, while the specific rheological profile and the temperature-dependent sol-gel transition of the polymer matrix ensures prolonged structural integrity and retention of C-SLNs at the application site. The sustained local release of curcumin, its strong anti-biofilm action when incorporated into SLNs coupled with its previously reported good antioxidant activity achieve the desired efficacy [17].

Studies describes that suitably designed nanostructures with integrative biopolymers derived from natural sources dramatically improve design-targeted antimicrobial actions and that natural biopolymer extracts, such as chitosan, have strong antibacterial properties [28]. In addition, sophisticated nanocomposites that are synthesized intelligently can show a significant level of antimicrobial activity [29]. Likewise, the careful design of the lipid matrix and temperature-responsive polymers in our C-SLN hydrogel ensures full expression of curcumin's

natural therapeutic qualities. This brings the sophisticated aspects of the technology one step closer to being a feasible clinical treatment for localized periodontitis.

3.5. Incorporation of C-SLNs into a hydrogel system

Poloxamer-based hydrogel systems are widely used for drug delivery owing to their unique properties of sol-gel transition regulated by temperature. Poloxamer 407 is widely used because of its in-situ gelling property with a change in temperature to > 30 °C [30]. Formulations based on poloxamer help improve retention at the application site, which is important for local drug delivery systems. It has been widely employed as a convenient dosage form for periodontitis [13]. However, poloxamer-based gels have weak gel strength and mucoadhesive properties in addition to rapid dissolution. Therefore, it has been suggested that other polymers, such as carbomer (Carbopol), alginate, chitosan, and polycarbophil, be used in combination with poloxamer. Based on this information, we decided to use a mixture of Poloxamer 407 and Carbopol 934 to develop a hydrogel system. The chosen concentrations of 10% Poloxamer 407 and 0.5% Carbopol 934 were based on the sol-gel transition and rheological and mucoadhesive profiles that were optimized in previous study [17]. We attempted the direct addition of poloxamer and Carbopol to the aqueous C-SLN dispersion; however, these polymers did not dissolve in the dispersion at the selected concentrations. Therefore, it was decided to develop the hydrogel separately (Fig. 7: A); however, the addition of C-SLN dispersion to the latter would lower the effective concentration of curcumin and the gelling polymers. Therefore, we lyophilized the C-SLNs (Fig. 7: B) and incorporated a suitable quantity into the hydrogel, resulting in an in-situ gelling system (Formulation A; Fig. 7: C-E)) containing a similar concentration of curcumin as originally included in the C-SLN dispersion (0.6% w/v curcumin). The size of C-SLNs was maintained upon redispersion in water after lyophilization (data not shown), even without the addition of a cryoprotectant. It is assumed that PEG 600 incorporated as a cosolvent during C-SLN manufacture also offers cryoprotection for lyophilization.

However, most studies have reported the use of curcumin at a concentration of 1% w/v, though in a free form (not nano-encapsulated) for periodontitis. Hence, we prepared a formulation in which a higher quantity of lyophilized C-SLNs was incorporated into the hydrogel system, resulting in a 1% w/v concentration of curcumin (Formulation B). However, this resulted in a very thick paste-like consistency, owing to the higher concentration of solids (~ 50%). The system was considerably stiffer than Formulation A and did not show sol consistency, even upon cooling (Fig. 7: F).

It is important to note that the curcumin concentration in Formulation A (0.6% w/v) was set to match the original concentration of C-SLN dispersion. Accordingly, Formulation A was considered the optimal dual delivery system for being the best compromise between stable NP drug loading, favorable rheological properties, and adequate syringeability for the proposed clinical use.

3.6. Comparative evaluation of formulation A and B: role of curcumin concentration and vehicle properties

Formulation A contains curcumin at 0.6% w/v, while Formulation B contains 1% w/v, in the same Carbopol-poloxamer hydrogel. These formulations were compared with respect to physicochemical, mechanical, and biological parameters as described below.

Total Drug Content: High and reproducible TDC values (Table 1) indicate the successful and reproducible method of preparation with minimal wastage.

Polydispersity index and particle size: Formulation A (C-SLNs dispersion at 0.6% w/v) exhibited a predominantly unimodal size distribution with an intensity peak at 618 ± 99 nm with a low PDI of 0.115 (Fig. 8), indicating a uniform particle population. The elevated hydrodynamic diameter than free C-SLNs dispersion (383 nm) is primarily attributed to the high viscosity of Carbopol-poloxamer matrix, which restricts Brownian motion and causes DLS to overestimate particle size, a well-recognized artifact in viscous media. Additional contribution from polymeric corona formation around the SLN surface also increases the measured hydrodynamic radius. The low PDI and smoothly decaying autocorrelation function together confirm that this size shift reflects physicochemical interaction rather than uncontrolled aggregation. In contrast, Formulation B displayed a broader, coarser distribution (833 ± 394 nm; PDI: 0.253), with a wider intensity histogram and less uniform autocorrelation decay, indicating greater polydispersity and a higher tendency toward aggregation reflecting inferior colloidal

Table 1
TDC values of formulations prepared on different occasions (n = 6).

S. No	Formulation	Curcumin concentration (% w/v)	TDC value (mg/mL)	% TDC
1	Formulation A	0.6	5.86 ± 0.07	97.64 ± 1.29
2	Formulation B	1	9.49 ± 0.10	94.90 ± 1.08

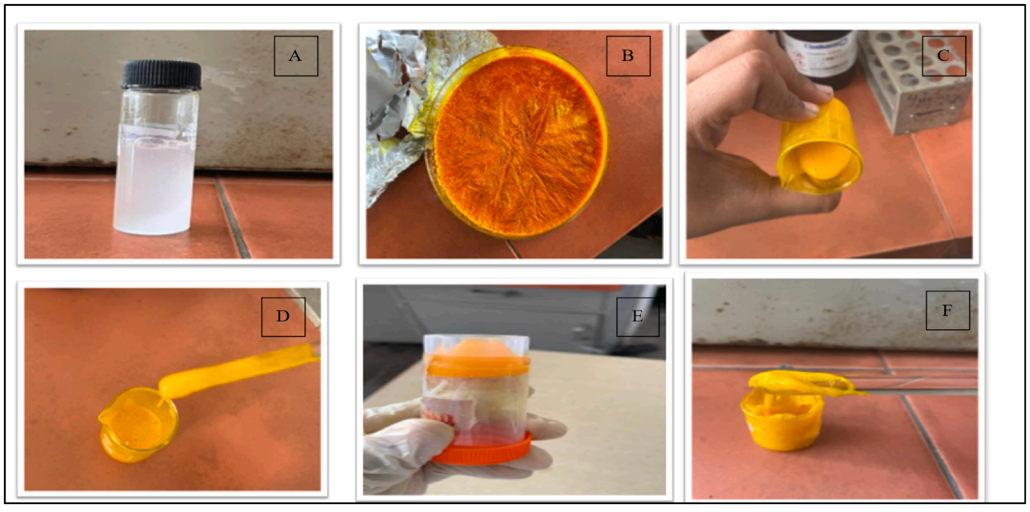

Fig. 7. Hydrogel formulations incorporating C-SLNs; (A) Blank hydrogel, (B) Lyophilized C-SLNs, (C) & (D) Formulation A showing fluidity, (E) sol to gel conversion of Formulation A upon warming, (F) Formulation B, which is stiff and not fluid.

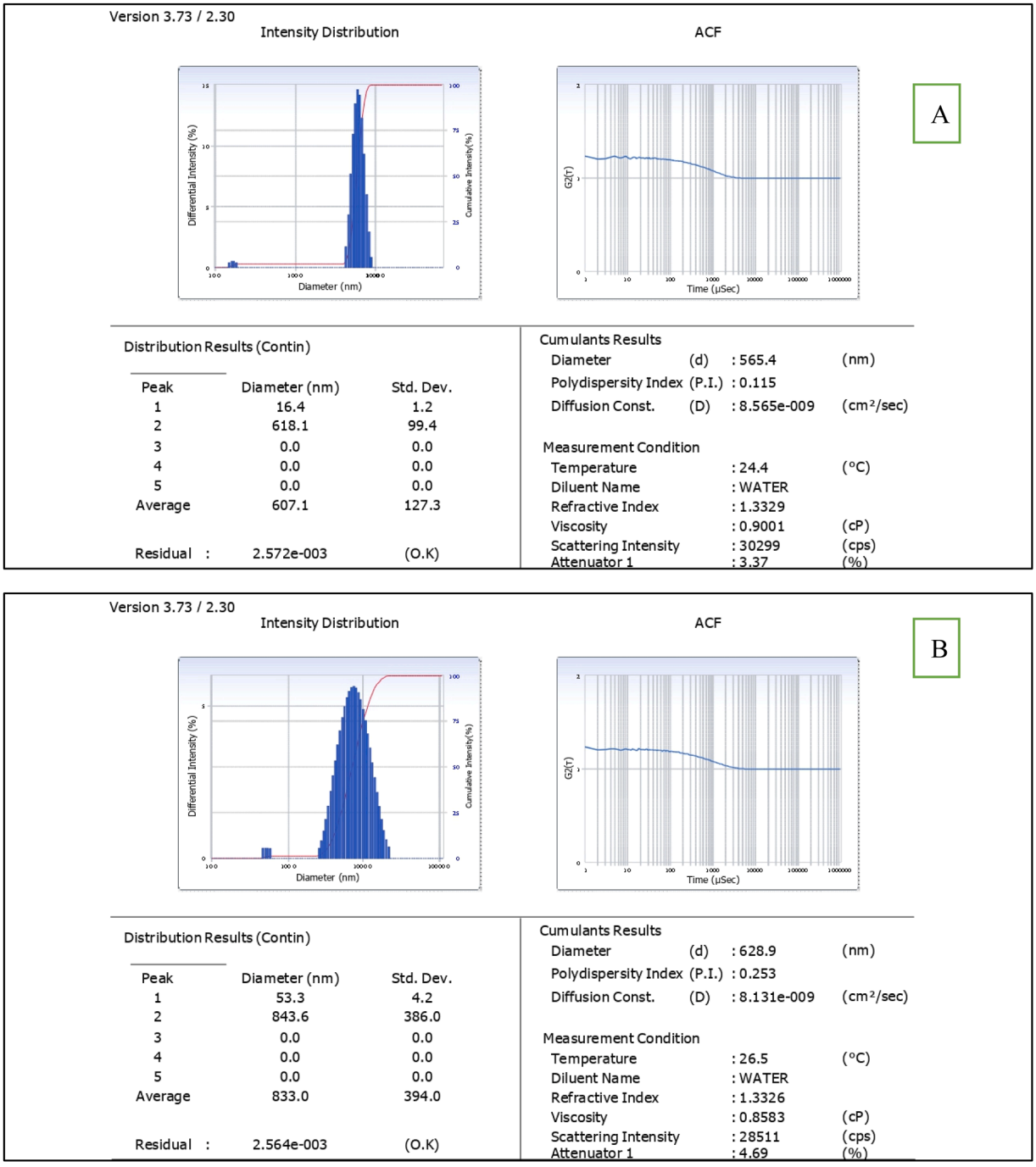

Fig. 8. Representative image of particle size for C-SLN loaded hydrogel formulation A and B.

homogeneity compared to Formulation A.

Determination of pH: The pH of prepared formulations A and B were in the desired range of 7.2 ± 0.082 and 6.9 ± 0.089, respectively. Curcumin is unstable at both acidic and alkaline pH, and its optimal pH is found to lie between 6.2 and 7.4 [31]. Furthermore, the near-neutral pH of the formulations will ensure that the patient does not experience irritation or discomfort of any kind upon application.

Autoclavability: As the formulation must be directly applied at the site of infection, it needs to be sterilized. The final hydrogel formulation, when autoclaved, was unstable, and the gel structure was disintegrated. Therefore, the components of the hydrogel system were sterilized separately, and the C-SLN dispersion was autoclaved separately. The latter has been established to be stable for autoclaving in an earlier study from our lab [18]. Sterilized and lyophilized C-SLNs were thus incorporated into the sterile aqueous dispersion of polymers. The hydrogel formulation thus developed was stable and retained all its properties.

Syringeability and sol-gel transition: Formulation A displayed perfect injectability with the ability of the substance to form a thermoreversible gel at the periodontal temperature (~32.71 ± 0.52°C). In contrast, Formulation B did not flow sufficiently from a 21-gauge needle at standard handling pressure.

Texture Analysis: Analysis of texture profile data provided information on the formulation dependent rheological data, which is shown in Table 2 and Fig. 9. C-SLN dispersion, in isolation, behaved as a very soft, and fluid-like system. This behaviour is as predicted, due to the C-SLNs dispersion lacking in structural stability and in adhesion. Blank

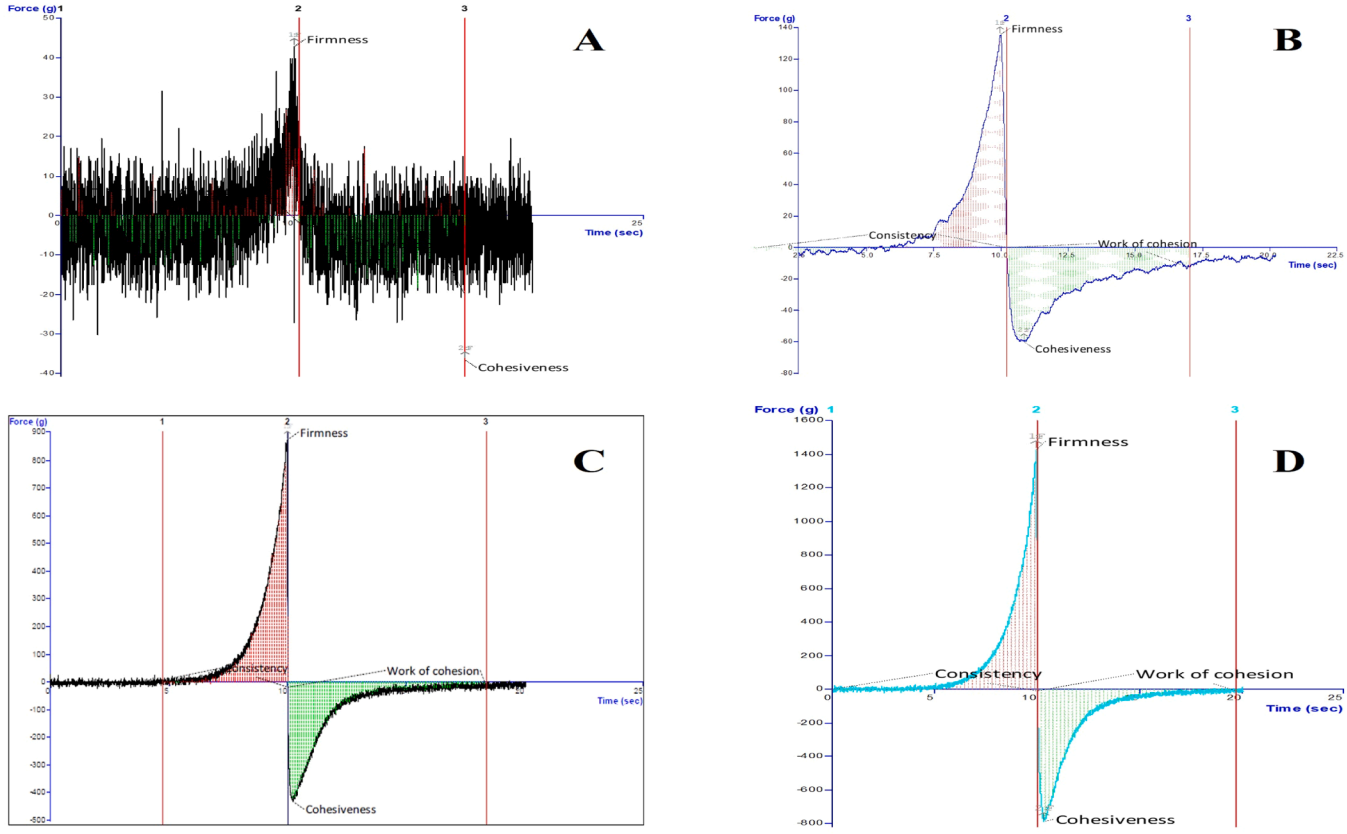

Fig. 9. Texture profile analysis plots of various samples A) C-SLN, B) blank hydrogel, C) Formulation A, D) Formulation B. Formulation A contains 0.6% w/v curcumin, whereas Formulation B contains 1% w/v curcumin as C-SLNs in the same Carbopol-poloxamer hydrogel vehicle.

hydrogel showed a minimal mechanical structure and the lyophilized C-SLNs improved the mechanical properties of the hydrogel considerably.

Formulation B was the stiffest, most stable, least cohesive, and had the highest work of cohesion of all the tested samples (Table 2). This implies a high structural density with cohesive and elastic properties, resulting in a very stiff structure. It also presented an overloaded network of polymers resulting in high resistance to probe withdrawal. Conversely, Formulation A presented low mechanical stability in comparison to Formulation B. C-SLN dispersion in Formulation A expressed a relatively stable network of low density in comparison to Formulation B. A trade-off between the formulations is evident, with formulation B being overly stiff with extreme cohesive and adhesive properties, while Formulation A being optimal in providing low resistance while offering firm consistency during application.

3.7. FESEM studies

The C-SLN hydrogel was examined at different magnifications (Fig. 10): 1.8 k × (Panel A) to view the hydrogel matrix, 3 k × (Panel B) to see SLNs within the hydrogel, and 70 k × (Panel C) to get a closer look at SLNs from the area highlighted in Panel B. In the polymeric hydrogel network (Panel A), a continuous porous structure was observed, along with a few distinct features. Through automated image analysis, four objects were detected, each with an equivalent diameter of 30 μm (in uncalibrated units) and an average aspect ratio (AR; minor/major) of 0.24 ± 0.32. This indicates that these features were more likely to be irregular structural components of the gel rather than distinct particles. Panel B demonstrated that SLNs were incorporated into the hydrogel's microstructure. Fourteen unique particles were counted, with their mean equivalent diameters being (10 μm) and their mean AR values being 0.32 ± 0.18. The high particle numbers and relatively higher AR values indicate the presence of well-shaped nanoparticles in the matrix, which is consistent with SLN structure. The high-magnification analysis presented in Panel C facilitated the identification of individual particles. Four particles were identified in the matrix, and their sizes were found to be around 500 nm based on the calibrated scale while their AR was in the range 0.46–0.71, with the mean being approximately 0.64 ± 0.12. The results clearly demonstrate that the C-SLNs incorporated into the hydrogel are almost near-spherical particles showing very minor deviations from isotropy. The FESEM images presented here reveal that C-SLNs are successfully incorporated into the hydrogel matrix.

Fig. 10 A describes hydrogel matrix, B represents SLNs enmeshed in the hydrogel matrix, C represents zoomed image of SLNs inside the hydrogel from image B.

Table 2
Texture profile analysis parameters of different formulations at 37°C.

Sample	Hardness (g)	Consistency (g.s)	Cohesiveness (g)	Work of Cohesion (g.s)
C-SLN dispersion	43.0	2.1	−36.6	−29.4
Blank hydrogel	135.7	139.9	−60.1	−178.5
Formulation A	883.6	801.7	−440.2	−718.3
Formulation B	1427.7	1543.2	−797.2	−1392.5

3.8. In vitro release

The *in vitro* release of curcumin from Formulations A and B was evaluated over 168 h (Fig. 11), and the profiles were modeled using zero-order, first-order, Higuchi, and Korsmeyer-Peppas (KP) equations. For both formulations, the Higuchi model provided the best fit,

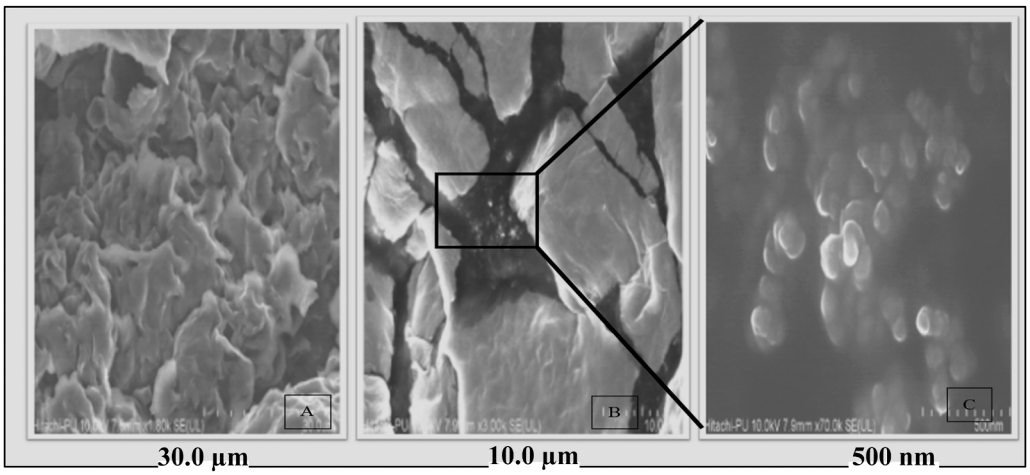

Fig. 10. FESEM images of C-SLN hydrogel at 1.8X (A), 3X (B) and 70X (C) magnification.

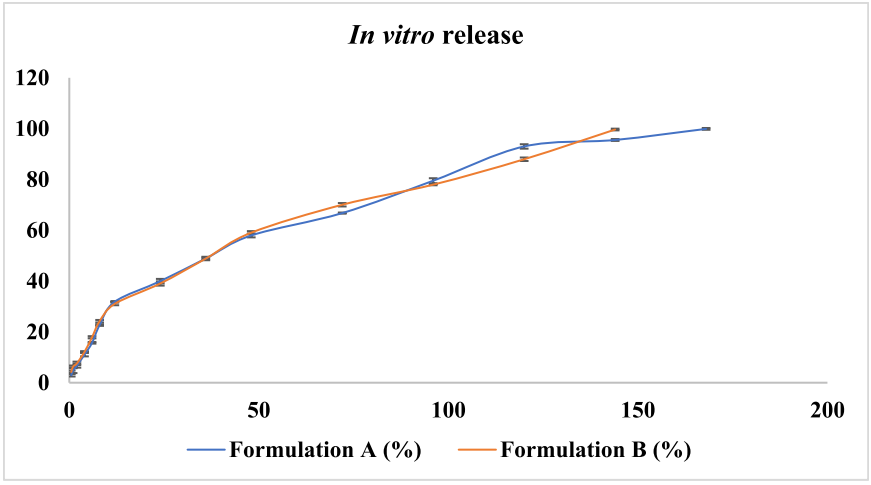

Fig. 11. Release (%) of curcumin from Formulation A and B (n = 6).

consistent with diffusion-controlled release from a matrix system: Formulation A, R^2= 0.993, and Formulation B, R^2= 0.996. Zero- and first-order fits were inferior (A: R^2=0.918 and 0.978; B: R^2=0.933 and 0.968). KP analysis limited to the initial region (<60% release) yielded n = 0.674, k = 0.0473, R^2= 0.967 for A and n = 0.597, k = 0.0604, R^2= 0.986 for B, indicating anomalous transport with a strong diffusion component. Similarity/dissimilarity testing across common time points (0.5–144 h) confirmed that the profiles were highly similar (f2 >50; f1 <15), and one-way ANOVA showed no significant difference between A and B at matched times ($p > 0.05$). Quantitatively, Formulation B released marginally faster than Formulation A up to 144 h, having released 99.65% against 95.54% of curcumin. After 168 h, A was found to have released up to 99.9% curcumin.

The Weibull model $F(t)= 1-\exp[-(t/\alpha)^{\beta}]$ was applied for a closer analysis of the release curves of Formulations A and B. Graphing ln[-ln (1-F)] versus ln(t) produced very good fits within the time range from 0.5 to 144 h. For Formulation A, the coefficients $\beta = 0.799$ and α= 48.90 h ($R^2 = 0.988$) point to a slow release associated with diffusion ($\beta < 1$). The time required for achieving nearly 63% release is about 49 h. The β value of 0.707 and α equal to 55.04 h ($R^2 = 0.990$) for Formulation B indicate a more pronounced delay in release rate with time, with a release time of about 55 h. The release kinetics of both profiles can be described by the Weibull model with $\beta < 1$, thus supporting diffusion control as found in the Higuchi and Korsmeyer-Peppas model analysis [18].

The addition of 50% v/v methanol to the dissolution medium was necessary to ensure sink conditions as curcumin is extremely hydrophobic, and to avoid its hydrolytic degradation as the study was run for 168 h. The use of this dissolution medium is previously described by us [16,17]. However, it must be emphasized that it is a non-physiological model and the effects of salivary flow, enzymatic digestion, and the dynamics of crevicular fluid are not described by it. Therefore, the rate of drug release may not actually match the clinical setting and is acknowledged as a limitation of the study.

3.9. *In vitro cytotoxicity studies*

C-SLNs and C-SLN hydrogel exhibited a viability between 69.01% and 100.00% in the MTT assay at concentrations equivalent to 20 µg/mL and 40 µg/mL of curcumin (Fig. 12).

In accordance with the ISO 10993–5 standards concerning the assessment of medical devices and biomaterials, a reduction in cell viability of 30% (i.e. maintaining ≥ 70% viability) is considered non-cytotoxic. C-SLN hydrogel showed a viability of 70.11 ± 1.82% even at the maximum tested concentration of 40 µg/mL meeting the ISO 10993–5 threshold.

3.10. *Preliminary clinical trial of prepared Formulation A*

Based on the physicochemical screening and formulation feasibility

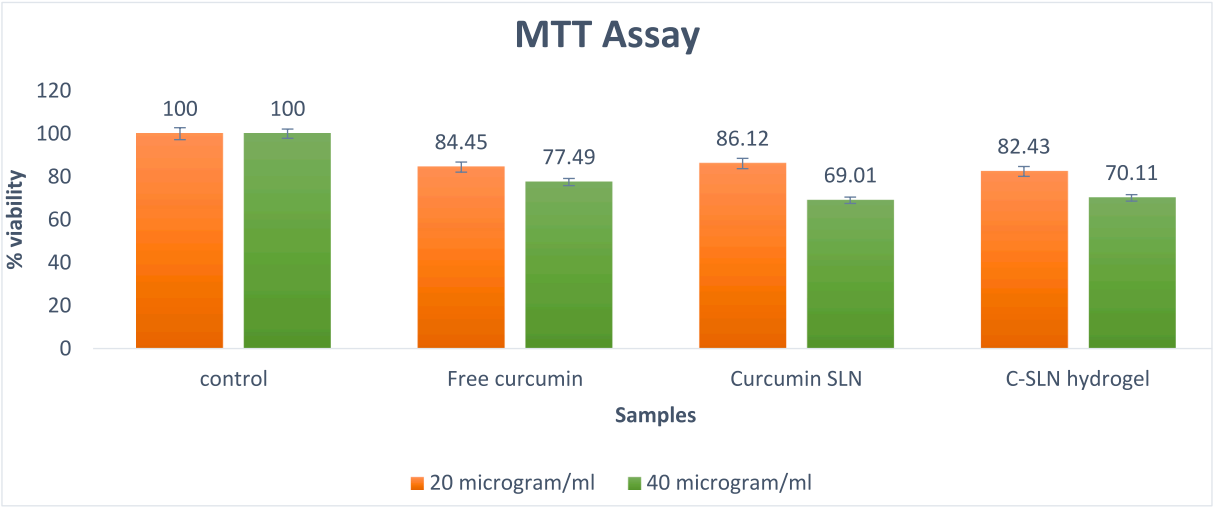

Fig. 12. Cytotoxicity of curcumin formulations by MTT assay in mammalian cells after 24 h at 20 and 40 μg/mL curcumin equivalent (mean ± SD, n = 3). Control viability remained ($p = 1.000$). Free curcumin showed ($p = 0.201$). Curcumin SLNs reduced viability ($p < 0.001$), and C-SLN hydrogel ($p = 0.007$), indicating significant, dose-dependent cytotoxicity for nanoparticle formulations while maintaining > 50% viability.

studies, only Formulation A containing 0.6% w/v curcumin was selected for clinical evaluation. Although Formulation B contained a higher curcumin concentration (1% w/v), its excessive viscosity, poor sol-gel behavior, and compromised syringeability rendered it unsuitable for subgingival application. The efficacy of curcumin as an adjunct anti-infective and anti-inflammatory to nonsurgical periodontal therapy (SRP) has been substantiated in systematic reviews and meta-analysis in terms of significant differences observed in gingival and sulcus bleeding indices [32]. The current study utilized improvised C-SLNs in combination with SRP for the management of periodontitis in a preliminary clinical investigation (Scheme 1) and revealed very encouraging findings. Mann-Whitney U and Wilcoxon W tests were applied for the statistical analysis. A statistically significant improvement was observed in the assessed clinical parameters of PD and CAL at all time points within the experimental and control groups ($p < 0.05$) (Table 3)

Intergroup comparison in the observed mean values for PD and CAL showed statistically significant improvement in the C-SLNs + SRP group at baseline, i.e., 0–1 month ($p = .037$ and.034), baseline to 3 months, and 1 month to 3 months (Table 4) [13,32]

To place the clinical findings of the present study in context, they are evaluated against three key bodies of evidence in the curcumin-based local drug delivery literature: the randomized controlled trials by Pérez-Pacheco et al. [15], the thermoresponsive curcumin gel studies by Nasra et al. [13] and Guru et al. [14] and the prior work from our own group, Oberoi et al. [17].

Among the most methodologically rigorous clinical investigations the randomized, double-blind, placebo-controlled split-mouth trial, evaluated a single local application of curcumin-loaded PLGA/PLA nanoparticles as an adjunct to SRP. The trial found no clinically significant improvements over placebo at six months, with the authors attributing this outcome to the single-application design, poor mucoadhesion of the nanoparticle suspension, and rapid clearance from the periodontal pocket [15]. A subsequent animal study from the same group reported that local curcumin-loaded PLGA/PLA nanoparticles improved periodontal tissue repair in vivo when retention was enhanced [33] These two studies together provided the primary rationale for the design of the C-SLN hydrogel system developed in the present work, which achieves a sustained drug release over seven days (168 h). The

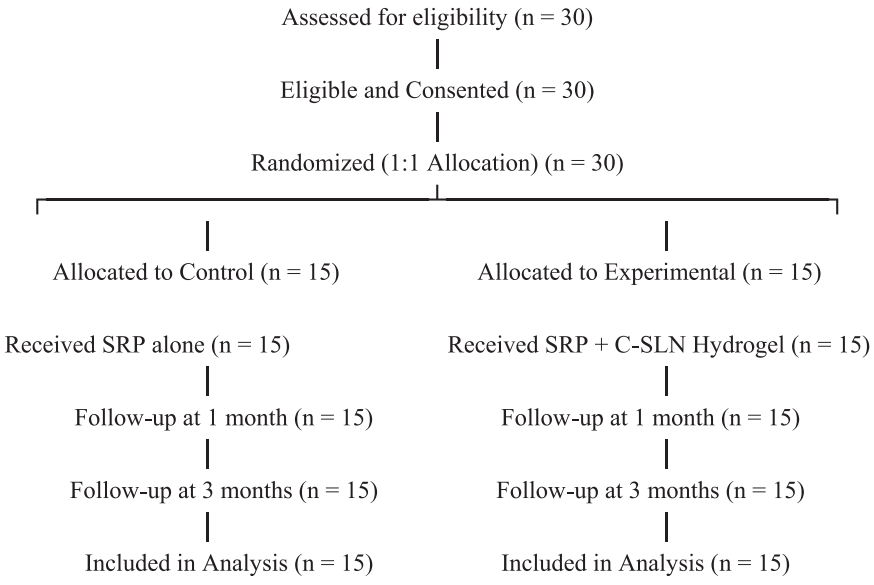

Scheme 1. The clinical study design describing SRP and SRP + C-SLN hydrogel treatment at the start of study following recruitment of patients.

Table 3
Intragroup and intergroup comparisons of clinical parameters at baseline, 1 and 3 months.

Clinical Parameter	Group	Baseline (Mean±SD)	1 Month (Mean±SD)	3 Months (Mean±SD)	BL vs 1 M	BL vs 3 M	1 M vs 3 M
Probing Depth (PD)	Experimental	4.000 ± 0.700	2.928 ± 0.424	1.794 ± 0.349	< 0.001***	0.001**	0.001**
	Control	3.523 ± 0.874	2.576 ± 0.574	2.053 ± 0.385	< 0.001***	0.001**	0.001**
	Intergroup P	0.051	0.037*	0.099	—	—	—
Clinical Attachment Level (CAL)	Experimental	4.078 ± 0.651	2.978 ± 0.389	1.975 ± 0.323	< 0.001***	0.001**	0.001**
	Control	3.630 ± 0.766	2.649 ± 0.529	1.967 ± 0.472	< 0.001***	0.001**	0.001**
	Intergroup P	0.077	0.034*	0.874	—	—	—

Values are expressed as Mean ± Standard Deviation (SD). BL = Baseline; 1 M = 1 Month; 3 M = 3 Months. BL vs 1 M, BL vs 3 M, and 1 M vs 3 M represent intragroup comparisons over time. Intergroup P values represent comparisons between the experimental and control groups at the same time point. *P < 0.05 indicates statistical significance; **P < 0.01 indicates highly significant difference; ***P < 0.001 indicates very highly significant difference.

Table 4
Intergroup comparison of the change in the parameters from baseline (BL) to 1 and 3 months.

Clinical Parameter	Group	BL−1 Month (Mean ± SD)	BL−3 Months (Mean ± SD)	1 Month−3 Months (Mean ± SD)
Change in Probing Depth (PD)	Experimental (SRP + C-SLNs)	1.072 ± 0.709	2.320 ± 0.733	1.093 ± 0.299
	Control (SRP)	0.946 ± 0.665	1.442 ± 0.750	0.403 ± 0.342
	P value*	0.315	0.003**	< 0.001**
Change in Clinical Attachment Level (CAL)	Experimental (SRP + C-SLNs)	1.100 ± 0.782	2.193 ± 0.773	0.933 ± 0.253
	Control (SRP)	0.981 ± 0.586	1.611 ± 0.659	0.635 ± 0.194
	P value*	0.376	0.034*	0.004**

Values are expressed as Mean ± Standard Deviation (SD).
P value indicates intergroup comparison between experimental and control groups.
*P < 0.05 significant; **P < 0.01 highly significant.

improved retention profile of the C-SLN hydrogel is proposed as the mechanism underlying the significant reductions in probing depth (PD) and gains in clinical attachment level (CAL) observed in the SRP + C-SLN hydrogel group relative to SRP alone. Repeated application protocols, planned for future investigations, are expected to further extend this therapeutic benefit.

The clinical evaluation of a free curcumin in-situ gel combining Poloxamer 407 and Carbopol for the treatment of periodontitis, reported a significant reduction in gingival index and pocket depth at one month [13]. Comparable clinical benefits were reported using a similar thermoresponsive curcumin gel formulation [14]. While these studies confirm the value of thermoresponsive curcumin systems, neither employed a nanoparticulate curcumin carrier. The reliance on free curcumin in conventional gel matrices limits cellular uptake, tissue penetration, and overall bioavailability. The present study advances upon these findings by demonstrating that encapsulation of curcumin within SLNs enhances its cellular uptake by 38-fold; this combined with a thermoresponsive hydrogel matrix, yields distinct biopharmaceutical advantages over free-drug gel systems. Additional value is offered by the inclusion of in vitro antibiofilm studies conducted against polymicrobial clinical periodontal isolates using an ex vivo dentin disc model, an assessment absent from both the Nasra and Samal studies.

The present study also builds directly upon our prior work [17] which focused on the preparation and physicochemical characterization of curcumin-loaded SLNs within an in-situ gelling system but did not include clinical evaluation. The present work advances the translational development of this formulation across five dimensions: (i) systematic comparison of two formulations (A: 0.6% w/v; B: 1% w/v curcumin) with respect to physicochemical, mechanical, and biopharmaceutical properties; (ii) antibiofilm activity against polymicrobial clinical periodontal isolates using an ex vivo dentin disc model; (iii) CLSM quantification of cellular uptake, demonstrating a 38-fold increase; (iv) cytotoxicity assessment confirming safety; and (v) a clinical evaluation in a cohort of 30 patients demonstrating marked improvements in PD and CAL. The present study therefore represents the first clinical assessment of this SLN-based formulation.

The clinical benefit observed here is further supported by the broader literature on adjunctive curcumin therapy. A systematic review and meta-analysis reported significant improvements in bleeding on probing and sulcular bleeding indices with curcumin used as an adjunct to SRP compared to SRP alone [32]. This adjunctive benefit is further amplified when curcumin is delivered via a nanotechnology-based platform. Notably, a 2% turmeric nanocarrier formulation evaluated in a randomized controlled clinical trial produced antimicrobial outcomes comparable to those of chlorhexidine gel, reinforcing the potential of nanostructured curcumin systems as clinically meaningful adjuncts to mechanical periodontal therapy.

Although the C-SLN hydrogel demonstrated significantly greater improvements in PD and CAL during the early healing phase, the intergroup differences became less pronounced at the three-month evaluation. This pattern suggests that the principal benefit of the hydrogel lies in accelerating the initial resolution of inflammation and promoting early periodontal healing, rather than in producing sustained superiority over the observation period. This temporal trend is biologically plausible: curcumin exerts potent anti-inflammatory, antioxidant, and antimicrobial effects during the early phases of wound healing, while both treatment groups continue to benefit from the sustained effects of SRP and natural periodontal tissue remodeling. As the hydrogel was administered only once at baseline, its pharmacological activity would be expected to diminish progressively over time. Repeated application protocols therefore warrant investigation in future randomized clinical trials to determine whether the early clinical advantage conferred by the C-SLN hydrogel can be sustained across longer follow-up periods.

4. Conclusions

SLN thermoresponsive curcumin hydrogel was developed and characterized for subgingival application. To our knowledge, this is the first study to assess the safety and antimicrobial activity of a curcumin loaded SLN based subgingival hydrogel. The C-SLN hydrogel showed no cytotoxicity against KB cells, simultaneously offering a 38-fold increase in cellular uptake and activity against biofilm of polymicrobial clinical isolates. Results from the Korsmeyer-Peppas and Higuchi analyses indicates anomalous, diffusion-controlled release extending to 168 h. The C-SLN hydrogel as an adjunct to SRP, in a 30 patient preliminary clinical study, resulted in greater reduction of probing depth and greater improvement of clinical attachment level, compared to the SRP alone, over a span of 3 months.

The SLN matrix confers superior colloidal stability, favourable rheological behaviour, and adequate syringeability, for Formulation A loading 0.6% w/v curcumin. Given that the C-SLN hydrogel, despite the controlled release for 7 days, is likely to be washed out of the periodontal pocket, it is suggested that the first clinical treatment is supplemented with additional sub-gingival treatment every two weeks by

the dentist or as a C-SLN hydrogel applied topically by the patient. It is anticipated that these treatment methods will provide improved outcomes and increased patient satisfaction. The favourable outcomes from this pilot clinical intervention study offers sound justification for additional studies in larger cohorts and with consecutive treatment cycles along with measurements of microbiological and inflammatory markers in the oral cavity. The combination of curcumin and rational delivery via nanotechnology offers a new approach that is cost-effective and will likely result in low levels of antimicrobial resistance.

CRediT authorship contribution statement

Aashi Bhardwaj: Methodology. **Jain Ashish:** Supervision. **Garima Sharma:** Methodology. **Bakr Ahmed:** Writing – original draft. **Pariksha Oberoi:** Methodology. **Navjot Sharma:** Writing – review & editing, Writing – original draft. **Praveen Rishi:** Supervision, Conceptualization. **Vishakha Grover:** Writing – original draft, Supervision, Conceptualization. **Shivam Gupta:** Writing – review & editing, Writing – original draft, Methodology. **Indu Pal Kaur:** Supervision, Conceptualization. **Arashdeep Kaur:** Methodology, Formal analysis. **Joga Singh:** Methodology. **Ohric Anchal:** Methodology.

Consent to participate

Dental plaque samples from individuals suffering from periodontal diseases were collected after obtaining written informed consent for voluntary participation.

Ethical Approval

Preliminary clinical studies were approved by the Institutional Human Ethics Committee of Panjab University PUIEC210312-III−045.

Funding

This study received no external funding.

Declaration of Competing Interest

The authors declare that they have no known competing financial interests or personal relationships that could have appeared to influence the work reported in this paper.

Acknowledgments

The authors acknowledge the equipment and other facilities outside of the DST-FIST, DST-Purse, DST-SAIF, and UGC-CAS facilities at UIPS and CIL, Panjab University.

Data availability

Not applicable.

References

[1] R. Saini, P. Marawar, S. Shete, S. Saini, Periodontitis, a true infection, J. Glob. Infect. Dis. 1 (2009) 149, https://doi.org/10.4103/0974-777x.56251.
[2] M.X. Chen, Y.J. Zhong, Q.Q. Dong, H.M. Wong, Y.F. Wen, Global, regional, and national burden of severe periodontitis, 1990–2019: An analysis of the Global Burden of Disease Study 2019, J. Clin. Periodontol. 48 (2021) 1165–1188, https://doi.org/10.1111/JCPE.13506;PAGE:STRING:ARTICLE/CHAPTER.
[3] C. Janakiram, A. Mehta, R. Venkitachalam, Prevalence of periodontal disease among adults in India: A systematic review and meta-analysis, J. Oral. Biol. Craniofac. Res. 10 (2020) 800–806, https://doi.org/10.1016/J.JOBCR.2020.10.016.
[4] S. S, D. Dhamodhar, P. D, R. M, S. R, N. P, Prevalence of periodontal diseases among general adult population in Tamil Nadu, India: A Cross-Sectional Fact-Finding study, Int. J. Chem. Biochem. Sci. 25 (2024), https://doi.org/10.62877/48-ijcbs-24-25-19-48.
[5] R. Mohanty, S.J. Asopa, M.D. Joseph, B. Singh, J.P. Rajguru, K. Saidath, U. Sharma, Red complex: Polymicrobial conglomerate in oral flora: A review, J. Fam. Med. Prim. Care 8 (2019) 3480, https://doi.org/10.4103/JFMPC.JFMPC_759_19.
[6] K.Y. How, K.P. Song, K.G. Chan, Porphyromonas gingivalis: An Overview of Periodontopathic Pathogen below the Gum Line, Front. Microbiol. 7 (2016) 53, https://doi.org/10.3389/FMICB.2016.00053.
[7] F.Q. Bui, C.L.C. Almeida-da-Silva, B. Huynh, A. Trinh, J. Liu, J. Woodward, H. Asadi, D.M. Ojcius, Association between periodontal pathogens and systemic disease, Biomed. J. 42 (2019) 27–35, https://doi.org/10.1016/j.bj.2018.12.001.
[8] A. Manohar, T. Suvarna, S.V. Prabhakar Vattikuti, B.A. Al-Asbahi, S. Sangaraju, N. Mameda, K.H. Kim, Synthesis, characterization and electrochemical properties of Ni0.4Mg0.6Fe2O4/CeO2/MnFe2O4 nanocomposite, Ceram. Int. 51 (2025) 6525–6532, https://doi.org/10.1016/J.CERAMINT.2024.12.096.
[9] A. Manohar, T. Suvarna, S.V. Prabhakar Vattikuti, P. Manivasagan, E.S. Jang, S. F. Shaikh, A. Kumar, K. Sharma, K.H. Kim, Development of MgFe2O4/ZnFe2O4/CeO2 nanocomposites: Exploration for electrochemical energy storage and biocompatible properties, Inorg. Chem. Commun. 172 (2025) 113736, https://doi.org/10.1016/J.INOCHE.2024.113736.
[10] L.M.G. Zambrano, D.A. Brandao, F.R.G. Rocha, R.P. Marsiglio, I.B. Longo, F. L. Primo, A.C. Tedesco, M.R. Guimaraes-Stabili, C. Rossa, Local administration of curcumin-loaded nanoparticles effectively inhibits inflammation and bone resorption associated with experimental periodontal disease, 2018 8:1, Sci. Rep. 8 (2018) 1–11, https://doi.org/10.1038/s41598-018-24866-2.
[11] S. Hewlings, D. Kalman, Curcumin: A Review of Its Effects on Human Health, Foods 6 (2017) 92, https://doi.org/10.3390/foods6100092.
[12] Y. Huang, Z. Huang, X. Zhang, H. Omidian, R.L. Wilson, S. Dey, C. Barry, J. Silverman, Enhancing Therapeutic Efficacy of Curcumin: Advances in Delivery Systems and Clinical Applications, 2023, Vol. 9, Page 596, Gels 9 (2023) 596, https://doi.org/10.3390/GELS9080596.
[13] M.M.A. Nasra, H.M. Khiri, H.A. Hazzah, O.Y. Abdallah, Formulation, in-vitro characterization and clinical evaluation of curcumin in-situ gel for treatment of periodontitis, Drug. Deliv. 24 (2017) 133–142, https://doi.org/10.1080/10717544.2016.1233591.
[14] S.R. Guru, K.Adithya Reddy, R.J. Rao, S. Padmanabhan, R. Guru, T.S. Srinivasa, Comparative evaluation of 2% turmeric extract with nanocarrier and 1% chlorhexidine gel as an adjunct to scaling and root planing in patients with chronic periodontitis: A pilot randomized controlled clinical trial, J. Indian. Soc. Periodontol. 24 (2020) 244–252, https://doi.org/10.4103/JISP.JISP_207_19.
[15] C.G. Pérez-Pacheco, N.A.R. Fernandes, F.L. Primo, A.C. Tedesco, E. Bellile, B. Retamal-Valdes, M. Feres, M.R. Guimarães-Stabili, C. Rossa, Local application of curcumin-loaded nanoparticles as an adjunct to scaling and root planing in periodontitis: Randomized, placebo-controlled, double-blind split-mouth clinical trial, Clin. Oral. Investig. 25 (2021) 3217–3227, https://doi.org/10.1007/S00784-020-03652-3.
[16] T. Gupta, J. Singh, S. Kaur, S. Sandhu, G. Singh, I.P. Kaur, Enhancing Bioavailability and Stability of Curcumin Using Solid Lipid Nanoparticles (CLEN): A Covenant for Its Effectiveness, Front. Bioeng. Biotechnol. 8 (2020) 1–14, https://doi.org/10.3389/fbioe.2020.00879.
[17] P. Oberoi, J. Singh, G. Sharma, V. Grover, I.P. Kaur, Preparation and Characterization of in-Situ Gelling Systems Containing Curcumin Loaded Solid Lipid Nanoparticles for Periodontitis, Curr. Trends Biomed. Eng. Biosci. 20 (2021) 1–19, https://doi.org/10.19080/CTBEB.2021.20.556032.
[18] S.K. Sandhu, S. Kumar, J. Raut, M. Singh, S. Kaur, G. Sharma, T.L. Roldan, S. Trehan, J. Holloway, G. Wahler, J.D. Laskin, P.J. Sinko, F. Berthiaume, B. Michniak-Kohn, P. Rishi, N. Ganesh, I.P. Kaur, Systematic Development and Characterization of Novel, High Drug-Loaded, Photostable, Curcumin Solid Lipid Nanoparticle Hydrogel for Wound Healing, Antioxidants 10 (2021) 725, https://doi.org/10.3390/antiox10050725.
[19] I.P. Kaur, V. Kakkar, P.K. Deol, M. Yadav, M. Singh, I. Sharma, Issues and concerns in nanotech product development and its commercialization, J. Control. Release 193 (2014) 51–62, https://doi.org/10.1016/J.JCONREL.2014.06.005.
[20] E. Giuliano, D. Paolino, M. Fresta, D. Cosco, Mucosal applications of poloxamer 407-based hydrogels: An overview, Pharmaceutics 10 (2018) 1–26, https://doi.org/10.3390/pharmaceutics10030159.
[21] D. Ramadon, Solid Lipid Nanoparticles (SLN): Formulation and Fabrication, Pharm. Sci. Res. 10 (2023), https://doi.org/10.7454/PSR.V10I2.1313.
[22] W. Wang, T. Chen, H. Xu, B. Ren, X. Cheng, R. Qi, H. Liu, Y. Wang, L. Yan, S. Chen, Q. Yang, C. Chen, Curcumin-Loaded Solid Lipid Nanoparticles Enhanced Anticancer Efficiency in Breast Cancer, Molecules 23 (2018) 1578, https://doi.org/10.3390/molecules23071578.
[23] B. Pitts, M.A. Hamilton, N. Zelver, P.S. Stewart, A microtiter-plate screening method for biofilm disinfection and removal, J. Microbiol. Methods 54 (2003) 269–276, https://doi.org/10.1016/S0167-7012(03)00034-4.
[24] I.R. Schmolka, Artificial skin I. Preparation and properties of pluronic F-127 gels for treatment of burns, J. Biomed. Mater. Res. 6 (1972) 571–582, https://doi.org/10.1002/jbm.820060609.
[25] A.K. Philip, K. Pathak, Osmotic flow through asymmetric membrane: A means for controlled delivery of drugs with varying solubility, AAPS PharmSciTech 7 (2006) E1–E11, https://doi.org/10.1208/pt070356.
[26] M. Li, J. Lv, Y. Yang, G. Cheng, S. Guo, C. Liu, Y. Ding, Advances of Hydrogel Therapy in Periodontal Regeneration-A Materials Perspective Review, Gels 8 (2022), https://doi.org/10.3390/GELS8100624.
[27] B. Yin, J.M. Dodda, S.H.D. Wong, G. Roshan Deen, J.S. Bate, A. Pachauri, B. Shiroud Heidari, T. Kovářík, C.A. Luo, S.W. Tsai, Smart injectable hydrogels for periodontal regeneration: Recent advancements in biomaterials and biofabrication

strategies, Mater. Today Bio 32 (2025) 101855, https://doi.org/10.1016/J.MTBIO.2025.101855.
[28] H. Hemmami, I. Ben Amor, S. Zeghoud, A. Ben Amor, S.E. Laouini, A. Alsalme, D. Cornu, M. Bechelany, A. Barhoum, Chitosan extraction from Amanita phalloides: yield, crystallinity, degree of deacetylation, azo dye removal and antibacterial properties, Front. Chem. 12 (2024) 1353524, https://doi.org/10.3389/FCHEM.2024.1353524/TEXT.
[29] R.Zouari Ahmed, S.E. Laouini, C. Salmi, A. Bouafia, S. Meneceur, H.A. Mohammed, S. Chihi, F. Alharthi, J.A.A. Abdullah, Green synthesis of α-Fe2O3 and α-Fe2O3@Ag NC for degradation of rose Bengal and antimicrobial activity, Biomass-.-. Convers. Biorefin 15 (2025) 255–269, https://doi.org/10.1007/S13399-023-05046-3/TABLES/4.
[30] G. Dumortier, J.L. Grossiord, F. Agnely, J.C. Chaumeil, A Review of Poloxamer 407 Pharmaceutical and Pharmacological Characteristics, Pharm. Res. 23 (2006) 2709–2728, https://doi.org/10.1007/s11095-006-9104-4.
[31] M. Kharat, Z. Du, G. Zhang, D.J. McClements, Physical and Chemical Stability of Curcumin in Aqueous Solutions and Emulsions: Impact of pH, Temperature, and Molecular Environment, J. Agric. Food Chem. 65 (2017) 1525–1532, https://doi.org/10.1021/acs.jafc.6b04815.
[32] Y. Zhang, L. Huang, J. Zhang, A.N. De Souza Rastelli, J. Yang, D. Deng, Anti-Inflammatory Efficacy of Curcumin as an Adjunct to Non-Surgical Periodontal Treatment: A Systematic Review and Meta-Analysis, Front. Pharmacol. 13 (2022) 808460, https://doi.org/10.3389/FPHAR.2022.808460/BIBTEX.
[33] C.G. Perez-Pacheco, N.A.R. Fernandes, A.C. Camilli, D.P. Ferrarezi, A.F. Silva, M. C. Zunareli, C.F. Amantino, F.L. Primo, M.R. Guimarães-Stabilli, C.R. Junior, Local administration of curcumin-loaded nanoparticles enhances periodontal repair in vivo, Naunyn. Schmiede Arch. Pharmacol. 396 (2023) 311–321, https://doi.org/10.1007/S00210-022-02310-7.